

SGOOD: SUBSTRUCTURE-ENHANCED GRAPH-LEVEL OUT-OF-DISTRIBUTION DETECTION

Zhihao Ding & Jieming Shi

The Hong Kong Polytechnic University

tommy-zh.ding@connect.polyu.hk

jieming.shi@polyu.edu.hk

ABSTRACT

Graph-level representation learning is important in a wide range of applications. However, existing graph-level models are generally built on i.i.d. assumption for both training and testing graphs, which is not realistic in an open world, where models can encounter out-of-distribution (OOD) testing graphs that are from different distributions unknown during training. A trustworthy model should not only produce accurate predictions for in-distribution (ID) data, but also detect OOD graphs to avoid unreliable prediction. In this paper, we present SGOOD, a novel graph-level OOD detection framework. We find that substructure differences commonly exist between ID and OOD graphs. Hence, SGOOD explicitly utilizes substructures to learn powerful representations to achieve superior performance. Specifically, we build a super graph of substructures for every graph, and design a two-level graph encoding pipeline that works on both original graphs and super graphs to obtain substructure-enhanced graph representations. To further distinguish ID and OOD graphs, we develop three graph augmentation techniques that preserve substructures and increase expressiveness. Extensive experiments against 10 competitors on numerous graph datasets demonstrate the superiority of SGOOD, often surpassing existing methods by a significant margin. The code is available at <https://anonymous.4open.science/r/SGOOD-0958>.

1 INTRODUCTION

Graphs are ubiquitous to represent complex data, *e.g.*, chemical compounds, proteins, and social networks. Graph-level representation learning is crucial for applications in biochemistry (Jiang et al., 2021; Rong et al., 2020), social network (Dou et al., 2021; Shao et al., 2017), natural language processing (Peng et al., 2018; Xu et al., 2019), and recommendation (Wu et al., 2014).

Existing graph-level learning models are based on the closed-world assumption, in which testing graphs encountered at deployment are drawn i.i.d. from the same distribution as the training graph data. However, in reality, the models are actually in an *open world*, where testing graphs can be from different distributions that are never exposed to the models during training. In other words, testing graphs can be out-of-distribution (OOD) *w.r.t.* in-distribution (ID) training graphs (Li et al., 2022a;b; Yang et al., 2022). Consequently, the models trained by ID data tend to be inaccurate when making predictions on OOD data (Hendrycks & Gimpel, 2017), which raises reliability concerns in safety-critical applications, *e.g.*, drug discovery (Basile et al., 2019). A trustworthy graph-level learning model should not only give accurate predictions for ID graphs, but also determine whether a test graph is OOD or not, to avoid unreliable predictions.

The key to graph-level OOD detection is capturing the structural differences that can help discern ID graphs and OOD graphs. As shown in our empirical study in Table 1, we find that *substructure differences of ID and OOD graphs commonly exist in real-world data*. (Dataset details in Section 4.)

Table 1: The percentage of OOD graphs with substructures never appeared in ID graphs.

Data	ENZYMES	IMDB-M	IMDB-B	BACE	BBBP	DrugOOD
	58.9%	14.0%	8.5%	50.0%	44.6%	77.3%

Specifically, we apply modularity-based community detection (Clauset et al., 2004) to detect the substructures of graphs in a dataset, and compute the percentage of OOD graphs with substructures that never appeared in ID graphs. In Table 1, the percentage is high, higher than 44% in 4 out of 6 datasets, indicating many OOD graphs contain substructures rarely in ID graphs.

The finding above justifies that, if one model can accurately preserve the substructures in ID graphs in an embedding space, intuitively, the model will give a large distance (i.e., OOD score) to OOD graphs with unseen substructures that are far away in the embedding space.

Explicitly leveraging substructure information is underexplored for graph-level OOD detection in the literature. As reviewed in Section 5, existing graph OOD detection methods, *e.g.*, (Li et al., 2022b; Liu et al., 2023b), mainly adopt message passing GNNs (Kipf & Welling, 2017; Hamilton et al., 2017) to first get node representations, and then generate graph-level representations solely based on these node representations. Their expressiveness is up-bounded by 1-WL (Weisfeiler-Leman) test and fails to extract crucial substructures like circles (Chen et al., 2020). There are hierarchical GNNs (Ying et al., 2018; Lee et al., 2019; Gao & Ji, 2019) and subgraph GNNs (Zhao et al., 2021; Zhang & Li, 2021) developed to explore high-order substructures. These methods are trained using ID graphs and classification loss with a focus on classification-related structures of ID graphs. However, for the problem of OOD detection, OOD graphs are unseen during training, and thus these methods may achieve sub-optimal OOD detection performance (Winkens et al., 2020), as shown in experiments.

We develop SGOOD, a novel framework that *explicitly* utilizes substructures and their relationships to learn *substructure-enhanced graph representations* for effective graph-level OOD detection. Specifically, we first build a super graph \mathcal{G}_i of substructures for every graph G_i to obtain substructures and their relationships. Then, a *two-level graph encoding pipeline* is designed to work on G_i and \mathcal{G}_i in sequence to learn expressive substructure-enhanced graph representations. We prove that SGOOD with the pipeline is strictly more expressive than 1&2-WL, which theoretically justifies the power of preserving substructure patterns for OOD detection. To further enhance the performance, we design three *substructure-preserving graph augmentation* techniques. The augmentation techniques utilize the super graph of substructures to ensure that the substructures in a graph are modified as a whole. The overall training objective of SGOOD combines a classification loss with a contrastive loss. At test time, given a graph G_i and its super graph \mathcal{G}_i , our OOD detector obtains the graph-level representations of both, which are then used for OOD score estimation. Extensive experiments are conducted to compare SGOOD against 10 baselines over many real-world graph datasets with various OOD types. SGOOD achieves superior performance, often outperforming existing methods by a significant margin. For instance, on an IMDB-M dataset, SGOOD achieves 9.58% absolute improvement in terms of AUROC over a runner-up baseline. In summary, our contributions are:

- We present SGOOD, a leading method that explicitly utilizes substructures and their relationships to learn expressive representations to effectively distinguish ID and OOD graphs in graph-level OOD detection.
- We design a novel two-level graph encoding pipeline by leveraging a constructed super graph of substructures, to empower SGOOD to learn substructure-enhanced graph representations.
- We further develop a collection of substructure-preserving graph augmentations via super graphs of substructures, to strengthen the distinguishability of SGOOD.
- Extensive experiments demonstrate the superiority of SGOOD for graph-level OOD detection.

2 PRELIMINARIES

We consider graph-level classification, which aims to classify a collection of graphs into different classes. Let $G_i = (V_i, E_i)$ be a graph, where V_i and E_i are node set and edge set, respectively. Let $\mathbf{x}_u \in \mathbb{R}^c$ denote the attribute vector of node $u \in V_i$ in graph G_i . from marginal distribution $\mathbb{P}_{\mathcal{X}}^{in}$. In summary, Denote \mathcal{X} as the in-distribution (ID) graph space and let $\mathcal{Y} = \{1, 2, \dots, C\}$ be the label space. In graph-level classification, the training set $D_{tr}^{in} = \{(G_i, y_i)\}_{i=1}^n$ is drawn i.i.d. from the joint data distribution $P_{\mathcal{X}\mathcal{Y}}$. Every graph sample in D_{tr}^{in} contains a graph G_i with label y_i . Let f be a learning model trained by the training set D_{tr}^{in} , and f is deployed to predict the label of a testing graph.

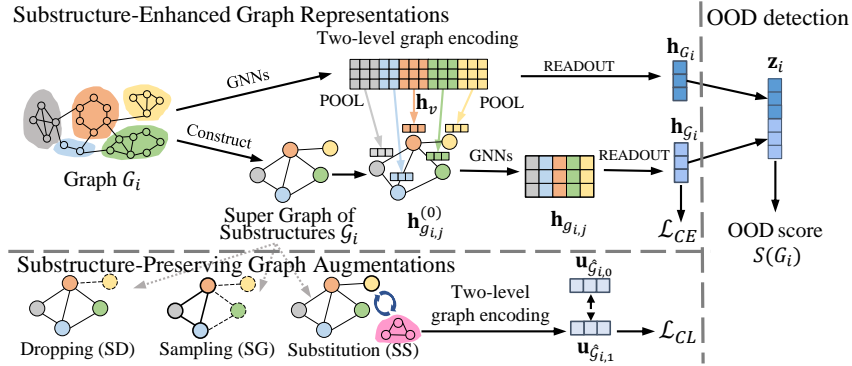


Figure 1: The SGOOD framework. SGOOD learns structure-enhanced graph representations via a super graph of substructures and two-level graph encoding. SGOOD further improves OOD separability by structure-preserving graph augmentations.

Graph-level Out-Of-Distribution Detection. At test time, graph-level OOD detection can be treated a task to decide whether a testing graph G_i in testing set D_{test} is from the ID $P_{\mathcal{X}}$ or from other irrelevant distributions (*i.e.*, OOD).

A typical way for OOD detection is to develop an OOD detector by leveraging the representations generated from the classification model f that is trained via ID training graphs in D_{tr}^{in} . Specifically, the OOD detector has a scoring function $S(G_i)$ for every testing graph $G_i \in D_{test}$. Testing graphs with low scores $S(G_i)$ are regarded as ID, while the graphs with high scores are OOD. As stated in (Ming et al., 2023), a score threshold λ is typically set so that a high fraction of ID data (*e.g.*, 95%) is correctly classified.

3 THE SGOOD METHOD

Solution Overview. Figure 1 illustrates the proposed SGOOD framework for graph-level OOD detection. SGOOD generates *substructure-enhanced graph representations*, and further improves representation quality by *substructure-preserving graph augmentations*. Specifically, given a graph G_i , we first detect its substructures and build its *super graph* \mathcal{G}_i , in which a super node represents a substructure in G_i and edges connect super nodes by following the connectivity in graph G_i . A *two-level graph encoding pipeline* is designed over both G_i and \mathcal{G}_i for graph-level representations that are enhanced by substructures. The training objective on ID training graphs is a cross-entropy loss \mathcal{L}_{CE} for graph classification. For augmentations, intuitively, if more information about training ID data is preserved, it is easier to distinguish unseen OOD data. The substructure-preserving graph augmentations are designed to achieve this. Specifically, given a graph G_i , we augment it by first performing dropping, sampling, and substitution on its super graph \mathcal{G}_i and then mapping the changes to G_i accordingly. This process is substructure-preserving in the sense that a substructure is modified as a whole. The overall training objective of SGOOD combines a classification loss \mathcal{L}_{CE} with a contrastive loss \mathcal{L}_{CL} . During test time, given a testing graph G_i , we first obtain the graph-level representations of both G_i and its super graph \mathcal{G}_i , concatenate and normalize the representations, and finally get OOD score $S(G_i)$. The pseudo-code of SGOOD is in Appendix D.

3.1 SUBSTRUCTURE-ENHANCED GRAPH REPRESENTATIONS

As mentioned, substructures in a graph are critical to distinguish the graph from others.

Given a graph G_i , we first describe how to construct its super graph \mathcal{G}_i of substructures, and then present a two-level graph encoding pipeline to generate substructure-enhanced graph representations.

Constructing a Super Graph of Substructures. Let a substructure $g_{i,j}$ of graph G_i be a connected subgraph of G_i . Specifically, a subgraph $g_{i,j} = (V_{i,j}, E_{i,j})$ is a substructure of $G_i = (V_i, E_i)$ iff $V_{i,j} \subseteq V_i$, $E_{i,j} \subseteq E_i$, and $g_{i,j}$ is connected. The substructures $\{g_{i,j}\}_{j=1}^{n_i}$ of a graph G_i satisfy the following properties: (i) the node sets of substructures are non-overlapping, (ii) the union of the nodes in all substructures is the node set of G_i , and (iii) every substructure is a connected subgraph of G_i .

Note that our framework SGOOD is orthogonal to existing subgraph detection methods (Dhillon et al., 2007; Cordasco & Gargano, 2010), and it is not our focus on how to detect subgraphs. By default, we use the off-the-shelf modularity-based community detection method (Clauset et al., 2004) to detect substructures considering modularity-based connectivity. In experiments, we also test other community/subgraph detection methods and find that the modularity-based substructures are effective in SGOOD, as shown in Table 6.

Then we construct the super graph \mathcal{G}_i by regarding every substructure $g_{i,j}$ as a super node in \mathcal{G}_i , and connect super nodes by inserting edges via Definition 1. Super graph \mathcal{G}_i can be regarded as a higher-order view that depicts the relationships between the substructures of a graph G . We also add self-loops in super graph \mathcal{G}_i .

Definition 1 (A Super Graph of Substructures). A super graph of substructures constructed from the input graph $G_i = (V_i, E_i)$ is denoted as $\mathcal{G}_i = (\mathcal{V}_i, \mathcal{E}_i)$, where every super node $g_{i,j}$ in node set $\mathcal{V}_i = \{g_{i,j}\}_{j=1}^{n_i}$ represents a substructure of G_i , and every edge in \mathcal{E}_i connecting two super nodes, and the edge set $\mathcal{E}_i = \{(g_{i,j}, g_{i,k}) | \exists u \in V_{i,j} \wedge v \in V_{i,k}, (u, v) \in E_i\}$.

Two-level Graph Encoding. Given a graph G_i and its super graph \mathcal{G}_i , we present a two-level graph encoding pipeline, as shown in Figure 1. The idea is that, in addition to learning representations over G_i , we further utilize the super graph \mathcal{G}_i to encode substructure information into graph representations, to better preserve distinguishable substructure patterns for effective OOD detection.

The two-level graph encoding first adopts GNNs to learn node representations with initial features over graph G_i . For every node $v \in V_i$, its representation $\mathbf{h}_v^{(l+1)}$ at $(l+1)$ -layer is obtained by Eq. (1). Different GNNs have different AGGREGATE and COMBINE. By default, we adopt Graph Isomorphism Network (GIN) (Xu et al., 2018) as the backbone. The GIN for graph G_i has L_1 layers.

$$\mathbf{h}_v^{(l+1)} = \text{COMBINE}^{(l+1)}(\mathbf{h}_v^{(l)}, \text{AGGREGATE}^{(l+1)}(\mathbf{h}_u^{(l)}, u \in N_{G_i}(v))), \mathbf{h}_v^{(0)} = \mathbf{x}_v, \quad (1)$$

where $\mathbf{h}_v^{(l)} \in \mathbb{R}^d$ is the intermediate representation of node v from the l -th layer GNNs with hidden dimension d , AGGREGATE^(l+1) is the function that aggregates node features from v 's neighborhood $N_{G_i}(v)$ in graph G_i , COMBINE^(l+1) is the function that updates node v 's representation by combining the representations of its neighbors with its own, and initially $\mathbf{h}_v^{(0)} = \mathbf{x}_v$.

Next, we obtain the representations of substructures $g_{i,j}$ in G_i by leveraging the node representations above. As shown in Eq. (2), given a node v , we first concatenate all representations $\mathbf{h}_v^{(l)}$ for $l = 1, \dots, L_1$ to get \mathbf{h}_v that preserves multi-scale semantics. Then, for a substructure $g_{i,j}$ of graph G_i , we obtain the substructure representation $\mathbf{h}_{g_{i,j}}^{(0)}$ by integrating \mathbf{h}_v of all v in $g_{i,j}$ via DeepSet pooling (Zhang et al., 2019) in Eq. (2).

$$\mathbf{h}_{g_{i,j}}^{(0)} = \text{POOL}(\{\mathbf{h}_v | v \in V_{i,j}\}), \mathbf{h}_v = \text{CONCAT}(\{\mathbf{h}_v^{(l)}\}_{l=1}^{L_1}) \quad (2)$$

Note that $\mathbf{h}_{g_{i,j}}^{(0)}$ only considers the nodes inside substructure $g_{i,j}$ and the original graph topology G_i . To further consider the relationships depicted in the super graph \mathcal{G}_i of substructures, we regard $\mathbf{h}_{g_{i,j}}^{(0)}$ as the initial features of super node $g_{i,j}$ in \mathcal{G}_i , and employ a L_2 -layer GIN over \mathcal{G}_i to learn substructure-enhanced graph representations by Eq. (3) and (4).

$$\mathbf{h}_{g_{i,j}}^{(l+1)} = \text{COMBINE}^{(l+1)}(\mathbf{h}_{g_{i,j}}^{(l)}, \text{AGGREGATE}^{(l+1)}(\mathbf{h}_{g_{i,k}}^{(l)}, g_{i,k} \in N_{\mathcal{G}_i}(g_{i,j}))), \quad (3)$$

where $N_{\mathcal{G}_i}(g_{i,j})$ contains the neighbors of super node $g_{i,j}$ in \mathcal{G}_i .

Lastly, in Eq. (4), we get the final representation $\mathbf{h}_{g_{i,j}}$ of every super node $g_{i,j}$ by concatenating the representation of $g_{i,j}$ in every layer of the L_2 -layer GIN, and finally obtain the graph representation $\mathbf{h}_{\mathcal{G}_i}$ by a readout function that is sum pooling.

$$\mathbf{h}_{\mathcal{G}_i} = \text{READOUT}(\{\mathbf{h}_{g_{i,j}} | g_{i,j} \in \mathcal{V}_i\}), \mathbf{h}_{g_{i,j}} = \text{CONCAT}(\{\mathbf{h}_{g_{i,j}}^{(l)}\}_{l=0}^{L_2}) \quad (4)$$

Remark that the representation $\mathbf{h}_{\mathcal{G}_i}$ of super graph \mathcal{G}_i of graph G_i is used to train the loss \mathcal{L}_{CE} for classification. Meanwhile, as explained shortly, for OOD detection during testing, we further consider another representation of graph G_i obtained by aggregating node representations as in Figure 1.

Discussion. In literature, there exist studies considering substructures/subgraphs for graph representation learning, such as hierarchical pooling (Ying et al., 2018; Lee et al., 2019; Gao & Ji, 2019) and subgraph GNNs (Zhang & Li, 2021; Zhao et al., 2021). We also conduct experiments to demonstrate that our SGOOD is more effective than these methods for the task of graph-level OOD detection.

3.2 SUBSTRUCTURE-PRESERVING GRAPH AUGMENTATIONS

Intuitively, if more information about training ID data is preserved, it is easier to distinguish unseen OOD data. Hence, we design substructure-preserving graph augmentations by leveraging the super graph \mathcal{G}_i of graph G_i , to improve the performance further.

However, it is challenging to achieve this. Substructures with subtle differences have different semantics. It is important to keep the substructures of a graph intact while performing augmentations. Common augmentation techniques like edge permutation and node dropping directly on graphs G_i may unexpectedly destroy meaningful substructures, and hamper OOD detection effectiveness.

To tackle the issue, we first perform augmentations on the super graph \mathcal{G}_i by regarding substructures as atomic nodes, and then map the augmentations to the original graph G_i with modifications over substructures as a whole. Specifically, we propose three substructure-level graph augmentations below, namely *substructure dropping (SD)*, *super graph sampling (SG)*, and *substructure substitution (SS)*. The default augmentation ratio is set to 0.3.

- *Substructure Dropping (SD)*. Given a graph G_i with its super graph \mathcal{G}_i , a fraction of super nodes in \mathcal{G}_i (i.e., the corresponding substructures in G_i) are discarded randomly. Remark that selected substructures are dropped as a whole.
- *Super Graph Sampling (SG)*. In the super graph \mathcal{G}_i , we start from a random node, sample a fixed-size connected subgraph in \mathcal{G}_i , and drop the rest nodes and edges. The changes are mapped to G_i accordingly. Depth-first search is chosen as the sampling strategy (You et al., 2020).
- *Substructure Substitution (SS)*. Given a graph G_i in class c with super graph \mathcal{G}_i of substructures, we randomly substitute a fraction of nodes in \mathcal{G}_i (i.e., substructures in G_i) with other substructures from the graphs of the same class c . To avoid drastic semantic change of the whole graph, only super nodes with degree one (excluding self-loops) in \mathcal{G}_i take part in the substitution.

3.3 OBJECTIVES AND TRAINING

For classification, we adopt a standard cross-entropy loss \mathcal{L}_{CE} . Specifically, after getting the representation $\mathbf{h}_{\mathcal{G}_i}$ for the super graph \mathcal{G}_i of graph G_i , we apply a linear transformation to get prediction logits \hat{y}_i , which is evaluated against the ground-truth class label y_i to get \mathcal{L}_{CE} by Eq. (5) for a mini-batch of B training graphs.

$$\mathcal{L}_{CE} = -\frac{1}{B} \sum_{i=1}^B \sum_{c=1}^C \mathbb{1}(y_i = c) \log(\hat{y}_{i,c}) \quad (5)$$

Then we adopt the substructure-preserving graph augmentations in Section 3.2 to get contrastive loss \mathcal{L}_{CL} . Specifically, given a mini-batch of B training graphs $\{G_i\}_{i=1}^B$ and their super graphs $\{\mathcal{G}_i\}_{i=1}^B$, we transform the super graphs to get $\hat{\mathcal{G}}_{i,0} = \mathcal{T}_0(\mathcal{G}_i)$ and $\hat{\mathcal{G}}_{i,1} = \mathcal{T}_1(\mathcal{G}_i)$, where \mathcal{T}_0 and \mathcal{T}_1 are two augmentations chosen among $\mathcal{A} = \{I, SD, SG, SS\}$, where I indicates no augmentation. Graph G_i is transformed accordingly via \mathcal{T}_0 and \mathcal{T}_1 to obtain $\hat{G}_{i,0}$ and $\hat{G}_{i,1}$ respectively. Then, the representations $\mathbf{h}_{\hat{\mathcal{G}}_{i,0}}$ and $\mathbf{h}_{\hat{\mathcal{G}}_{i,1}}$ of the two augmented super graphs can be calculated by applying Eq.(1)-(4). We transform $\mathbf{h}_{\hat{\mathcal{G}}_{i,0}}$ and $\mathbf{h}_{\hat{\mathcal{G}}_{i,1}}$ by a shared projection head $\psi(\cdot)$, which is a 2-layer MLP, followed by l_2 -normalization, to obtain $\mathbf{u}_{\hat{\mathcal{G}}_{i,0}} = \psi(\mathbf{h}_{\hat{\mathcal{G}}_{i,0}}) / \|\psi(\mathbf{h}_{\hat{\mathcal{G}}_{i,0}})\|$ and $\mathbf{u}_{\hat{\mathcal{G}}_{i,1}} = \psi(\mathbf{h}_{\hat{\mathcal{G}}_{i,1}}) / \|\psi(\mathbf{h}_{\hat{\mathcal{G}}_{i,1}})\|$, respectively. We get \mathcal{L}_{CL} by

$$\mathcal{L}_{CL} = \frac{1}{2B} \sum_{i=1}^B \sum_{a \in \{0,1\}} -\log \frac{\exp(\mathbf{u}_{\hat{\mathcal{G}}_{i,a}}^\top \mathbf{u}_{\hat{\mathcal{G}}_{i,1-a}} / \tau)}{\sum_{j=1}^B \exp(\mathbf{u}_{\hat{\mathcal{G}}_{i,a}}^\top \mathbf{u}_{\hat{\mathcal{G}}_{j,1-a}} / \tau) + \sum_{j=1}^B \mathbb{1}(j \neq i) \exp(\mathbf{u}_{\hat{\mathcal{G}}_{i,a}}^\top \mathbf{u}_{\hat{\mathcal{G}}_{j,a}} / \tau)}, \quad (6)$$

where τ is a temperature parameter.

Table 2: Data Statistics.

Dataset	Graph Type	OOD Type	# Class	# ID Train	# ID Val	# ID Test	# OOD Test
ENZYMES (Morris et al., 2020)	Proteins	Unseen Classes	6	480	60	60	60
IMDB-M (Morris et al., 2020)	Social Networks	Unseen Classes	3	1200	150	150	150
IMDB-B (Morris et al., 2020)	Social Networks	Unseen Classes	2	800	100	100	100
REDDIT-12K (Yanardag & Vishwanathan, 2015)	Social Networks	Unseen Classes	11	6997	875	875	875
BACE (Wu et al., 2018)	Molecules	Scaffold	2	968	121	121	121
BBBP (Wu et al., 2018)	Molecules	Scaffold	2	1303	164	164	164
DrugOOD (Ji et al., 2022)	Molecules	Protein Target	2	800	100	100	100
HIV (Wu et al., 2018)	Molecules	Scaffold	2	26319	3291	3291	3291

The overall training loss is

$$\mathcal{L} = \mathcal{L}_{CE} + \alpha \mathcal{L}_{CL}, \text{ where } \alpha \text{ is a weight factor.} \quad (7)$$

The training procedure of SGOOD consists of two stages. In the first pre-training stage, the parameters are solely updated by minimizing \mathcal{L}_{CL} for T_{PT} epochs. In the second stage, the parameters are fine-tuned under the combined overall loss \mathcal{L} for T_{FT} epochs. This training procedure achieves better performance than directly training \mathcal{L} , as shown in Appendix Figure 4 when pretraining T_{PT} is 0.

3.4 GRAPH-LEVEL OOD SCORING

Recall that the main goal of OOD detection is to let the representations of ID data and OOD data to be distant from each other. In terms of distance, at test time, given a testing graph $G_i \in D_{test}$, we use the standard Mahalanobis distance (Lee et al., 2018) to quantify its OOD score. If G_i is with large Mahalanobis distance from the ID training data in the embedding space, it tends to be OOD.

In SGOOD shown in Figure 1, in addition to the representation \mathbf{h}_{G_i} of the super graph \mathcal{G}_i of a testing graph G_i , we also aggregate the node representations of G_i to get $\mathbf{h}_{G_i} = \text{READOUT}(\{\mathbf{h}_v | v \in V_i\})$. Representations \mathbf{h}_{G_i} and \mathbf{h}_{G_i} are concatenated together to estimate the OOD score $S(G_i)$

$$S(G_i) = \max_{c \in [C]} (\mathbf{z}_i - \boldsymbol{\mu}_c)^\top \widehat{\Sigma}^{-1} (\mathbf{z}_i - \boldsymbol{\mu}_c), \quad (8)$$

$$\boldsymbol{\mu}_c = \frac{1}{N_c} \sum_{j: y_j=c} \mathbf{z}_j; \widehat{\Sigma} = \frac{1}{N} \sum_{c \in [C]} \sum_{j: y_j=c} (\mathbf{z}_j - \boldsymbol{\mu}_c)(\mathbf{z}_j - \boldsymbol{\mu}_c)^\top; \mathbf{z}_i = \frac{\text{CONCAT}(\mathbf{h}_{G_i}, \mathbf{h}_{G_i})}{\|\text{CONCAT}(\mathbf{h}_{G_i}, \mathbf{h}_{G_i})\|_2}, \quad (9)$$

where $[C] = \{1, 2, \dots, C\}$, $\boldsymbol{\mu}_c$ is the estimated class centroid for class c , and $\widehat{\Sigma}$ is the estimated covariance matrix for ID graphs.

3.5 ANALYSIS

We show in Proposition 1 that SGOOD is more expressive than 1&2-WL, indicating that SGOOD can distinguish more structural patterns, which, together with our empirical findings in Section 1, explains the power of SGOOD for graph-level OOD detection. The proof is provided in Appendix A.

Proposition 1. When the GNNs adopted in SGOOD are with sufficient number of layers, and the `POOL` function in Eq.(2) and `READOUT` function in Eq.(4) are injective, then SGOOD is strictly more powerful than 1&2-WL.

4 EXPERIMENTS

Datasets and Evaluation Metrics. We adopt real datasets that encompass diverse types of OOD graphs, as listed in Table 2. The OOD graph data is generated following (Liu et al., 2023b; Li et al., 2022b). All ID graphs D^{in} are randomly split into training, validation, and testing with ratio 8:1:1, following the settings of standard graph classification (Hu et al., 2020; Morris et al., 2020). The testing set consists of the same number of ID graphs and OOD graphs. We use three commonly used metrics AUROC, AUPR and FPR95 for OOD detection evaluation (Hendrycks & Gimpel, 2017; Wu et al., 2022). All these metrics are independent of threshold choosing. For the classification performance in ID graphs, we use Accuracy (ID ACC). Remark that the priority of the graph-level OOD detection task is to accurately identify OOD graphs, when maintaining instead of improving the ID ACC. The details of dataset descriptions and the metric formula are provided in Appendix B.1.

Table 3: Overall OOD detection performance by AUROC, AUPR, and FPR95 in percentage % (mean \pm std). \uparrow indicates larger values are better and vice versa. **Bold**: best. Underline: runner-up.

Method	ENZYMES			IMDB-M			IMDB-B			REDDIT-12K		
	AUROC \uparrow	AUPR \uparrow	FPR95 \downarrow	AUROC \uparrow	AUPR \uparrow	FPR95 \downarrow	AUROC \uparrow	AUPR \uparrow	FPR95 \downarrow	AUROC \uparrow	AUPR \uparrow	FPR95 \downarrow
MSP	61.34 \pm 3.79	61.65 \pm 6.64	89.67 \pm 2.26	42.75 \pm 1.52	51.04 \pm 1.93	95.73 \pm 1.63	58.13 \pm 2.31	59.63 \pm 1.22	91.40 \pm 4.16	50.63 \pm 0.87	48.60 \pm 1.08	95.95 \pm 1.25
Energy	54.69 \pm 9.18	56.90 \pm 8.85	89.33 \pm 3.55	24.50 \pm 19.73	37.26 \pm 11.78	96.40 \pm 2.25	49.58 \pm 17.76	59.03 \pm 13.06	92.80 \pm 3.55	55.10 \pm 0.48	56.52 \pm 0.78	97.19 \pm 0.58
ODIN	63.70 \pm 2.70	65.72 \pm 4.77	92.66 \pm 3.26	40.12 \pm 2.96	50.08 \pm 2.44	96.66 \pm 1.03	58.25 \pm 2.94	61.36 \pm 0.49	92.20 \pm 2.92	51.74 \pm 2.03	54.53 \pm 1.26	96.45 \pm 0.73
MAH	67.37 \pm 3.67	63.81 \pm 2.15	83.33 \pm 9.60	<u>69.26\pm3.67</u>	63.64\pm2.14	<u>60.93\pm9.06</u>	76.77 \pm 4.37	76.88 \pm 6.30	<u>81.40\pm7.14</u>	<u>72.68\pm0.87</u>	<u>74.47\pm0.48</u>	<u>80.75\pm2.05</u>
GNNSafe	56.85 \pm 8.91	56.13 \pm 8.26	97.00 \pm 3.71	21.93 \pm 1.76	36.88 \pm 1.68	95.46 \pm 1.42	70.49 \pm 14.80	75.67 \pm 15.71	87.80 \pm 5.81	51.68 \pm 0.08	53.97 \pm 0.52	95.59 \pm 2.80
GraphDE	61.35 \pm 3.99	66.26 \pm 2.98	99.00 \pm 0.81	66.87 \pm 4.25	62.60 \pm 4.47	93.06 \pm 8.24	26.91 \pm 3.35	42.73 \pm 2.06	100.00 \pm 0.00	59.40 \pm 0.18	63.06 \pm 0.30	81.82 \pm 0.01
GOOD-D	67.21 \pm 6.41	64.86 \pm 6.32	82.33 \pm 8.31	61.89 \pm 4.87	<u>66.91\pm7.60</u>	95.20 \pm 4.55	52.58 \pm 10.21	55.69 \pm 10.56	99.20 \pm 1.00	56.11 \pm 0.10	59.56 \pm 0.16	93.67 \pm 0.34
OCGIN	68.11 \pm 4.61	68.90 \pm 4.19	89.67 \pm 3.70	47.51 \pm 9.47	50.76 \pm 4.53	98.27 \pm 17.70	60.78 \pm 5.21	57.80 \pm 5.10	8780 \pm 9.15	59.33 \pm 1.26	60.02 \pm 1.88	90.00 \pm 2.01
GLocalKD	71.46 \pm 3.21	64.93 \pm 4.44	<u>78.67\pm6.37</u>	19.82 \pm 1.57	35.39 \pm 0.49	98.27 \pm 1.13	<u>79.39\pm4.71</u>	85.56\pm3.33	87.40 \pm 5.42	49.60 \pm 0.16	51.75 \pm 0.72	97.60 \pm 0.35
OGGTL	<u>73.22\pm1.83</u>	73.61\pm3.19	82.33 \pm 2.70	54.07 \pm 12.93	58.20 \pm 7.86	86.40 \pm 6.49	37.39 \pm 18.82	47.11 \pm 14.06	98.80 \pm 2.40	51.62 \pm 0.019	53.33 \pm 0.01	96.79 \pm 0.06
SGOOD	74.40\pm1.42	<u>72.53\pm2.51</u>	73.66\pm7.03	78.84\pm2.00	72.54\pm3.21	45.46\pm6.62	80.41\pm3.16	<u>83.49\pm3.59</u>	81.20\pm2.28	74.95\pm0.79	74.93\pm0.93	75.17\pm2.72
Method	BACE			BBBP			DrugOOD			HIV		
	AUROC \uparrow	AUPR \uparrow	FPR95 \downarrow	AUROC \uparrow	AUPR \uparrow	FPR95 \downarrow	AUROC \uparrow	AUPR \uparrow	FPR95 \downarrow	AUROC \uparrow	AUPR \uparrow	FPR95 \downarrow
MSP	46.34 \pm 6.10	48.65 \pm 3.08	97.02 \pm 2.18	57.37 \pm 4.28	56.84 \pm 3.36	94.63 \pm 2.26	52.86 \pm 5.26	54.49 \pm 4.33	98.80 \pm 0.01	50.75 \pm 1.88	50.49 \pm 0.91	95.52 \pm 0.50
Energy	46.05 \pm 6.66	49.68 \pm 4.16	97.36 \pm 2.92	56.56 \pm 4.16	55.74 \pm 2.78	92.68 \pm 2.62	52.81 \pm 5.36	54.98 \pm 4.36	98.20 \pm 1.16	50.97 \pm 2.13	50.49 \pm 0.91	95.50 \pm 0.59
ODIN	45.51 \pm 3.85	48.28 \pm 3.76	97.02 \pm 1.53	54.78 \pm 3.46	54.63 \pm 3.69	96.34 \pm 1.80	51.09 \pm 3.79	52.70 \pm 2.66	99.00 \pm 1.09	50.16 \pm 0.73	49.95 \pm 0.58	94.60 \pm 1.07
MAH	73.78 \pm 1.97	75.33 \pm 2.32	86.78 \pm 6.32	53.77 \pm 4.27	52.57 \pm 3.81	93.29 \pm 2.51	66.90 \pm 4.14	64.30 \pm 4.43	<u>81.60\pm4.58</u>	<u>58.10\pm3.60</u>	<u>57.18\pm3.18</u>	<u>91.89\pm1.32</u>
GNNSafe	47.61 \pm 7.50	51.52 \pm 5.91	98.18 \pm 2.05	47.04 \pm 2.40	51.52 \pm 5.90	98.41 \pm 0.99	50.44 \pm 0.57	51.14 \pm 0.30	96.01 \pm 0.33	50.98 \pm 6.82	55.13 \pm 6.81	96.01 \pm 0.33
GraphDE	47.32 \pm 1.52	51.11 \pm 2.57	94.21 \pm 4.58	50.88 \pm 2.78	51.47 \pm 3.84	94.63 \pm 2.34	60.19 \pm 4.32	62.59 \pm 2.47	88.80 \pm 5.60	52.38 \pm 1.86	54.14 \pm 3.21	94.89 \pm 0.84
GOOD-D	70.42 \pm 2.22	73.21 \pm 3.34	88.26 \pm 1.78	54.15 \pm 1.10	58.58 \pm 1.93	99.39 \pm 0.41	60.52 \pm 3.33	63.09 \pm 2.54	98.40 \pm 1.27	59.69 \pm 0.62	57.10 \pm 1.4	92.03 \pm 0.61
OCGIN	59.71 \pm 5.20	61.43 \pm 5.18	93.39 \pm 4.44	47.78 \pm 5.72	47.27 \pm 2.98	94.76 \pm 2.70	57.95 \pm 5.80	59.50 \pm 7.00	94.20 \pm 3.12	54.06 \pm 0.47	52.14 \pm 0.26	92.81 \pm 1.01
GLocalKD	45.34 \pm 2.11	55.39 \pm 2.35	98.68 \pm 1.11	43.77 \pm 2.23	45.84 \pm 1.20	98.29 \pm 1.00	45.72 \pm 0.97	50.90 \pm 3.33	100.00 \pm 0.00	46.81 \pm 2.90	46.95 \pm 2.01	97.05 \pm 0.19
OGGTL	<u>80.84\pm2.00</u>	<u>79.93\pm1.26</u>	<u>66.44\pm8.89</u>	<u>58.73\pm2.19</u>	60.47\pm1.38	<u>91.46\pm2.21</u>	<u>67.59\pm7.93</u>	<u>70.90\pm5.80</u>	83.00 \pm 11.22	51.78 \pm 0.19	53.71 \pm 0.22	96.41 \pm 0.05
SGOOD	84.39\pm2.73	83.32\pm2.49	64.13\pm4.83	61.25\pm1.60	<u>59.36\pm2.39</u>	88.04\pm3.44	73.15\pm4.48	73.25\pm4.49	67.40\pm5.16	60.82\pm0.75	59.99\pm0.69	90.39\pm1.04

Baselines and Implementation Details. We compare SGOOD with 10 competitors in 3 categories.

(i) General OOD detection methods, including

MSP (Hendrycks & Gimpel, 2017), *Energy* (Liu et al., 2020), *ODIN* (Liang et al., 2018), and *MAH* (Lee et al., 2018), for each of which, we replace their network backbone with GIN to handle graph data. (ii) Existing graph-level OOD detection methods, including *GNNSafe* (Wu et al., 2022), *GraphDE* (Li et al., 2022b) and *GOOD-D* (Liu et al., 2023b). (iii) Existing graph-level anomaly detection methods, including *OCGIN* (Zhao & Akoglu, 2021), *OCGTL* (Qiu et al., 2022), and *GLocalKD* (Ma et al., 2022). In SGOOD, we set the number of layers $L_1 = 3$ and $L_2 = 2$, and dimension d as 16. We use mini-batch gradient descent to optimize parameters in SGOOD with Adam optimizer, and batch size is set as 128. In SGOOD, we set T_{PT} as 100 epochs and T_{FT} as 500 epochs. In the first stage of training, learning rate is tuned in $\{0.01, 0.001, 0.0001\}$. For the second stage, we set learning rate as 0.001 and α as 0.1. On each dataset, we repeat experiments 5 times with different random seeds and report the mean metrics.

The implementation details of baselines are in Appendix B.3.

4.1 OVERALL GRAPH-LEVEL OOD DETECTION EFFECTIVENESS

Table 3 reports the overall graph-level OOD detection performance of all methods by AUROC, AUPR and FPR95 metrics on all datasets, by mean and standard deviation values. Observe that SGOOD consistently achieves superior OOD detection effectiveness under most settings. For instance, on IMDB-M, SGOOD has AUROC 78.84%, which indicates 9.58% absolute improvement over the best competitor with AUROC 69.26%. As another example on BACE molecule dataset, the AUROC of SGOOD is 84.39%, while the runner-up achieves AUROC 80.84%. The overall results in Table 3 demonstrate the power of our technical designs in SGOOD presented in Section 3 for graph-level OOD detection. Due to space limit, ID ACC results are in Appendix Table 9.

4.2 MODEL ANALYSIS

Ablation. In Table 4, SGOOD\A is SGOOD that ablates all augmentations in Section 3.2, i.e., $\alpha=0$ in Eq. (7); SGOOD (base) further ablates all substructure-related representations

in Section 3.1. In Table 4, first observe that, from SGOOD (base) to SGOOD\A and then to the complete version SGOOD, the performance gradually increases on all datasets, validating the effectiveness of all proposed techniques. Second, SGOOD\A already surpasses the best baseline performance on most datasets, which demonstrates the effect of the techniques in Section 3.1, without the augmentation techniques in Section 3.2. With the help of the substructure-preserving graph augmentations, SGOOD pushes the performance further higher.

In Figure 2, we visualize the ID and OOD score distributions of SGOOD (base), SGOOD\A and SGOOD on DrugOOD, with their mean scores shown in dotted lines. Clearly, we are obtaining more separable OOD scores against ID data from left to right in Figure 2, which demonstrates that our techniques in SGOOD can learn distinguishable representations for ID and OOD graphs.

Effect of Substructure-Preserving Graph Augmentations. We evaluate the augmentations (SD, SG, and SS) in Section 3.2, with conventional graph augmentations that are not substructure-preserving, including edge perturbation (EP), attribute masking (AM), node dropping (ND), and subgraph sampling (SA). Table 5 reports the results, AM is not applicable on IMDB-M and IMDB-B since they do not have node attributes. Observe that our SD, SG, and SS are the top-3 ranked techniques for graph-level OOD detection, validating the effectiveness of the proposed substructure-preserving graph augmentations. In Appendix Figure 6, we also visualize the improvements of all pairwise combinations of our augmentation techniques.

Effect of Substructure Extraction Methods. As mentioned, SGOOD is orthogonal to specific substructure extraction methods. Here in SGOOD, we evaluate several commonly-used methods to extract substructures, including Graclus (Dhillon et al., 2007), label propagation (LP) (Cordasco & Gargano, 2010), and BRICS (Degen et al., 2008). Specifically, BRICS uses Chemistry knowledge for extraction. In Table 6, SGOOD with different substructure detections are all better than SGOOD *w.o.* using substructures, and SGOOD with Modularity is the best. The results validate the effectiveness of our framework that leverages substructures for OOD detection.

Comparison with Subgraph-aware Models. We then compare SGOOD directly with subgraph-aware models, including three hierarchical pooling methods (SAG (Lee et al., 2019), TopK (Gao & Ji, 2019), DiffPool (Ying et al., 2018)) and two subgraph GNNs (NGNN (Zhang & Li, 2021) and GNN-AK⁺ (Zhao et al., 2021)). Note that these methods are not specifically designed for graph-level OOD detection. At test time, we extract the graph representations generated by these methods and use Mahalanobis distance as OOD score. Table 7 reports the AUROC results. SGOOD performs best on 5 out of 6 datasets and is the top-2 on DrugOOD. This validates the effectiveness of our substructure-related techniques in Section 3 for graph-level OOD detection.

Varying L_1 and L_2 . In the experiments above,

Table 4: Ablation AUROC (%)

Method	ENZYMES	IMDB-M	IMDB-B	BACE	BBBP	DrugOOD
Best baseline	71.46	69.26	<u>79.39</u>	73.78	57.37	57.37
SGOOD (base)	67.38	69.26	76.80	73.78	53.77	66.90
SGOOD\A	<u>73.60</u>	<u>75.22</u>	77.80	<u>75.96</u>	<u>57.84</u>	<u>68.80</u>
SGOOD	74.41	78.84	80.42	84.40	61.25	73.16

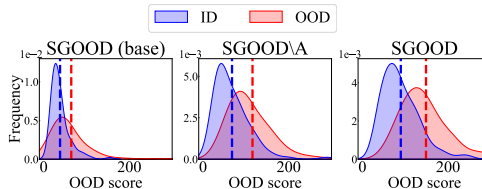


Figure 2: ID and OOD score distributions with the dotted line indicating the mean of ID/OOD scores.

Table 5: Comparing with different augmentations by AUROC (%)

	ENZYMES	IMDB-M	IMDB-B	BACE	BBBP	DrugOOD	Avg. Rank
EP	74.28	76.50	78.44	78.75	58.24	71.32	4.67
AM	72.44	/	/	77.28	59.68	71.27	5.25
ND	73.11	77.09	78.40	78.79	58.59	69.48	4.83
SA	72.12	76.76	79.25	77.13	57.84	72.66	4.83
SD	74.77	78.15	79.54	82.00	59.76	72.65	1.83
SG	72.74	77.98	78.97	82.24	59.58	71.97	3.33
SS	74.27	76.20	80.50	83.53	63.53	71.94	2.67

Table 6: Comparison between different substructure detection methods by AUROC (%).

SGOOD	ENZYMES	IMDB-M	IMDB-B	BACE	BBBP	DrugOOD
<i>w.o.</i> substructures	67.38	69.26	76.8	73.78	53.77	66.90
Modularity	74.41	78.84	80.42	84.40	61.25	73.16
Graclus	<u>71.12</u>	74.64	<u>78.86</u>	<u>79.54</u>	56.62	67.94
LP	68.09	<u>75.48</u>	78.46	76.63	54.90	<u>68.95</u>
BRICS	/	/	/	78.39	<u>60.18</u>	64.78

Table 7: Comparing with subgraph-aware models AUROC (%). **Bold**: best. Underline: runner-up.

Method	ENZYMES	IMDB-M	IMDB-B	BACE	BBBP	DrugOOD
SAG	70.40	76.50	77.30	<u>76.90</u>	<u>58.90</u>	65.80
TopK	70.20	<u>76.80</u>	77.20	74.20	54.90	58.50
DiffPool	73.30	75.90	78.00	76.50	57.50	70.60
NGNN	70.30	71.20	76.60	71.20	52.60	75.60
GNN-AK ⁺	68.50	73.50	77.20	70.90	54.30	63.00
SGOOD	74.41	78.84	80.42	84.40	61.25	<u>73.16</u>

we fix the layers of the two GINs in the two-level graph encoding in Section 3.1 to be $L_1 = 3$ and $L_2 = 2$ as default. If we search L_1 and L_2 , it is possible to get even better OOD detection results, as shown in Table 8 where L_1 and L_2 are varied with their sum fixed to be 5. For example, on BACE with $L_1=2$ and $L_2=3$, AUROC is 62.26%, about 1% higher than the default setting.

Efficiency. The training and inference time is in Appendix Table 11. SGOOD is faster to train than existing graph-level OOD detection methods, including GraphDE and GOOD-D, and has close efficiency with OCGIN and GLocalKD. SGOOD also has close training time to general OOD detection methods. All methods have close inference time.

Table 8: Varying L_1 and L_2 in SGOOD (AUROC).

L_1	L_2	ENZYMES	IMDB-M	IMDB-B	BBBBP	BACE	DrugOOD
4	1	74.00	77.13	81.00	80.43	62.00	71.17
3	2	74.41	78.84	80.42	84.40	61.25	73.16
2	3	73.63	76.03	79.05	80.34	62.26	69.12
1	4	74.22	77.83	76.79	76.62	61.08	68.01

More experiments. In Appendix, we compare the performance of SGOOD and baselines when different backbones other than GIN are used in Table 10, evaluate the effect when varying augmentation ratio in Figure 3, study the effect of pretraining epochs T_{PT} in Figure 4, vary the weight of contrastive loss α in Figure 5, and visualize detected substructures in Figure 7.

5 RELATED WORK

Graph-level Representation Learning. Graph-level representation learning aims to learn representations of entire graphs (Wu et al., 2020). GNNs (Hamilton et al., 2017; Kipf & Welling, 2017; Veličković et al., 2018; Xu et al., 2018) are often adopted (Guo et al., 2023; Yang et al., 2022) to first learn node representations by message passing on graphs and then node representations are aggregated by pooling functions to get graph-level representations (Liu et al., 2023a). It is shown that the expressiveness of such a way is limited by 1-WL (Chen et al., 2020; Li et al., 2020). Hence, there are general subgraph-aware methods to improve the expressive power, *e.g.*, hierarchical pooling (Gao & Ji, 2019; Lee et al., 2019; Ying et al., 2018) and subgraph GNNs (Zhang & Li, 2021; Zhao et al., 2021). Hierarchical pooling methods learn to assign nodes into different clusters and coarsen graphs hierarchically. Subgraph GNNs apply message passing on extracted rooted-subgraphs of nodes in a graph, and then aggregate subgraph representations (Frasca et al., 2022). Wang et al. (2022) assumes pre-defined repetitive type of substructures on periodic graphs. Contrarily, we do not have such an assumption and consider various substructures automatically extracted by community detection. Still, these methods assume that graphs are i.i.d in training and testing. In experiments, SGOOD is more effective for graph-level OOD detection.

Out-of-distribution Detection. OOD detection has received great research attention in various data domains, as learning models tend to be over-confident on out-of-distribution data (Hendrycks & Gimpel, 2017; Nguyen et al., 2015). There are OOD detection methods designed for image data (Hendrycks & Gimpel, 2017; Lee et al., 2018; Liang et al., 2018; Liu et al., 2020; Ming et al., 2023; Sehwag et al., 2021; Sun et al., 2022). Some methods rely on classification probabilities predicted by neural networks to get OOD scores (Hendrycks & Gimpel, 2017; Liang et al., 2018; Liu et al., 2020), while the others measure OOD scores according to the distance between test samples and ID training data (Lee et al., 2018; Ming et al., 2023; Sehwag et al., 2021; Sun et al., 2022). Note that non-graph OOD detection methods are designed without considering the unique characteristics of graphs, though they can be modified to handle OOD detection on graph data. As shown in our experiments, SGOOD surpasses these methods. Recently, several OOD detection methods on graphs have been proposed. Wu et al. (2022) explore node-level OOD detection by using energy function to detect OOD nodes in a graph, which is a different problem from this paper. For graph-level OOD detection, Li et al. (2022b) design a generative model that has the ability to identify outliers in training graph samples, as well as OOD samples during the testing stage. Liu et al. (2023b) develop a self-supervised learning approach to train their model to estimate OOD scores at test time. Recently, Zhang et al. (2022) proposes to learn anomalous substructures using deep random walk kernel, which depends on labeled anomalous graphs, while OOD graphs are unseen during the training stage and only available during the testing stage. Observe that existing graph-level OOD detection methods mainly leverage node representations output by GNNs (Kipf & Welling, 2017; Veličković et al., 2018; Xu et al., 2018) to get graph-level representations, while the rich substructure patterns hidden in

graphs are under-investigated for graph-level OOD detection. On the other hand, our method SGOOD explicitly uses substructures in graphs to learn high-quality graph-level representations for effective graph-level OOD detection. The representations generated by SGOOD are able to distinguish ID and OOD graphs with better performance than existing methods, as demonstrated in the extensive experiments.

6 CONCLUSION

We study the problem of graph-level OOD detection, and present a novel SGOOD method with superior performance. The design of SGOOD is motivated by the exciting finding that substructure differences commonly exist between ID and OOD graphs. By leveraging substructures, SGOOD aims to preserve more distinguishable graph-level representations between ID and OOD graphs. Specifically, we build a super graph of substructures for every graph, and develop a two-level graph encoding pipeline to obtain high-quality structure-enhanced graph representations. We theoretically prove the expressiveness power of the obtained representations. To further improve the representation quality, we develop a set of substructure-preserving graph augmentations. Extensive experiments on real-world graph datasets validate the superior performance of SGOOD over existing methods for graph-level OOD detection.

REFERENCES

- Anna O Basile, Alexandre Yahi, and Nicholas P Tatonetti. Artificial intelligence for drug toxicity and safety. *Trends in pharmacological sciences*, 40(9):624–635, 2019.
- Ulrik Brandes, Daniel Delling, Marco Gaertler, Robert Gorke, Martin Hoefer, Zoran Nikoloski, and Dorothea Wagner. On modularity clustering. *IEEE transactions on knowledge and data engineering*, 20(2):172–188, 2007.
- Zhengdao Chen, Lei Chen, Soledad Villar, and Joan Bruna. Can graph neural networks count substructures? *Advances in Neural Information Processing Systems*, 33:10383–10395, 2020.
- Aaron Clauset, Mark EJ Newman, and Cristopher Moore. Finding community structure in very large networks. *Physical review E*, 70(6):066111, 2004.
- Gennaro Cordasco and Luisa Gargano. Community detection via semi-synchronous label propagation algorithms. In *2010 IEEE international workshop on: business applications of social network analysis (BASNA)*, pp. 1–8. IEEE, 2010.
- Jörg Degen, Christof Wegscheid-Gerlach, Andrea Zaliani, and Matthias Rarey. On the art of compiling and using ‘drug-like’ chemical fragment spaces. *ChemMedChem: Chemistry Enabling Drug Discovery*, 3(10):1503–1507, 2008.
- Inderjit S Dhillon, Yuqiang Guan, and Brian Kulis. Weighted graph cuts without eigenvectors a multilevel approach. *IEEE transactions on pattern analysis and machine intelligence*, 29(11):1944–1957, 2007.
- Yingtong Dou, Kai Shu, Congying Xia, Philip S Yu, and Lichao Sun. User preference-aware fake news detection. In *Proceedings of the 44th International ACM SIGIR Conference on Research and Development in Information Retrieval*, pp. 2051–2055, 2021.
- Fabrizio Frasca, Beatrice Bevilacqua, Michael Bronstein, and Haggai Maron. Understanding and extending subgraph gnns by rethinking their symmetries. *Advances in Neural Information Processing Systems*, 35:31376–31390, 2022.
- Hongyang Gao and Shuiwang Ji. Graph u-nets. In *international conference on machine learning*, pp. 2083–2092. PMLR, 2019.
- Zhichun Guo, Bozhao Nan, Yijun Tian, Olaf Wiest, Chuxu Zhang, and Nitesh V Chawla. Graph-based molecular representation learning. In *Proceedings of the Thirty-Second International Joint Conference on Artificial Intelligence*, 2023.

-
- William L Hamilton, Rex Ying, and Jure Leskovec. Inductive representation learning on large graphs. In *Advances in Neural Information Processing Systems*, pp. 1025–1035, 2017.
- Dan Hendrycks and Kevin Gimpel. A baseline for detecting misclassified and out-of-distribution examples in neural networks. In *5th International Conference on Learning Representations*, 2017.
- Weihua Hu, Matthias Fey, Marinka Zitnik, Yuxiao Dong, Hongyu Ren, Bowen Liu, Michele Catasta, and Jure Leskovec. Open graph benchmark: Datasets for machine learning on graphs. *Advances in Neural Information Processing Systems*, 33:22118–22133, 2020.
- Yuanfeng Ji, Lu Zhang, Jiaxiang Wu, Bingzhe Wu, Long-Kai Huang, Tingyang Xu, Yu Rong, Lanqing Li, Jie Ren, Ding Xue, et al. Drugood: Out-of-distribution (ood) dataset curator and benchmark for ai-aided drug discovery—a focus on affinity prediction problems with noise annotations. *arXiv preprint arXiv:2201.09637*, 2022.
- Dejun Jiang, Zhenxing Wu, Chang-Yu Hsieh, Guangyong Chen, Ben Liao, Zhe Wang, Chao Shen, Dongsheng Cao, Jian Wu, and Tingjun Hou. Could graph neural networks learn better molecular representation for drug discovery? a comparison study of descriptor-based and graph-based models. *Journal of cheminformatics*, 13(1):1–23, 2021.
- Thomas N. Kipf and Max Welling. Semi-supervised classification with graph convolutional networks. In *International Conference on Learning Representations*, 2017.
- Junhyun Lee, Inyeop Lee, and Jaewoo Kang. Self-attention graph pooling. In *International conference on machine learning*, pp. 3734–3743. PMLR, 2019.
- Kimin Lee, Kibok Lee, Honglak Lee, and Jinwoo Shin. A simple unified framework for detecting out-of-distribution samples and adversarial attacks. *Advances in Neural Information Processing Systems*, 31, 2018.
- Haoyang Li, Xin Wang, Ziwei Zhang, and Wenwu Zhu. Ood-gnn: Out-of-distribution generalized graph neural network. *IEEE Transactions on Knowledge and Data Engineering*, 2022a.
- Pan Li, Yanbang Wang, Hongwei Wang, and Jure Leskovec. Distance encoding: Design provably more powerful neural networks for graph representation learning. *Advances in Neural Information Processing Systems*, 33:4465–4478, 2020.
- Zenan Li, Qitian Wu, Fan Nie, and Junchi Yan. Graphde: A generative framework for debiased learning and out-of-distribution detection on graphs. *Advances in Neural Information Processing Systems*, 35:30277–30290, 2022b.
- Shiyu Liang, Yixuan Li, and R Srikant. Enhancing the reliability of out-of-distribution image detection in neural networks. In *International Conference on Learning Representations*, 2018.
- Chuang Liu, Yibing Zhan, Chang Li, Bo Du, Jia Wu, Wenbin Hu, Tongliang Liu, and Dacheng Tao. Graph pooling for graph neural networks: Progress, challenges, and opportunities. In *Proceedings of the Thirty-Second International Joint Conference on Artificial Intelligence*, 2023a.
- Weitang Liu, Xiaoyun Wang, John Owens, and Yixuan Li. Energy-based out-of-distribution detection. *Advances in Neural Information Processing Systems*, 33:21464–21475, 2020.
- Yixin Liu, Kaize Ding, Huan Liu, and Shirui Pan. Good-d: On unsupervised graph out-of-distribution detection. In *Proceedings of the Sixteenth ACM International Conference on Web Search and Data Mining*, pp. 339–347, 2023b.
- Rongrong Ma, Guansong Pang, Ling Chen, and Anton van den Hengel. Deep graph-level anomaly detection by glocal knowledge distillation. In *Proceedings of the Fifteenth ACM International Conference on Web Search and Data Mining*, pp. 704–714, 2022.
- Yifei Ming, Yiyun Sun, Ousmane Dia, and Yixuan Li. How to exploit hyperspherical embeddings for out-of-distribution detection? In *The Eleventh International Conference on Learning Representations*, 2023.

-
- Christopher Morris, Nils M Kriege, Franka Bause, Kristian Kersting, Petra Mutzel, and Marion Neumann. Tudataset: A collection of benchmark datasets for learning with graphs. *arXiv preprint arXiv:2007.08663*, 2020.
- Anh Nguyen, Jason Yosinski, and Jeff Clune. Deep neural networks are easily fooled: High confidence predictions for unrecognizable images. In *Proceedings of the IEEE conference on computer vision and pattern recognition*, pp. 427–436, 2015.
- Hao Peng, Jianxin Li, Yu He, Yaopeng Liu, Mengjiao Bao, Lihong Wang, Yangqiu Song, and Qiang Yang. Large-scale hierarchical text classification with recursively regularized deep graph-cnn. In *Proceedings of the 2018 world wide web conference*, pp. 1063–1072, 2018.
- Chen Qiu, Marius Kloft, Stephan Mandt, and Maja Rudolph. Raising the bar in graph-level anomaly detection. In *Proceedings of the Thirty-First International Joint Conference on Artificial Intelligence*, 2022.
- Yu Rong, Yatao Bian, Tingyang Xu, Weiyang Xie, Ying Wei, Wenbing Huang, and Junzhou Huang. Self-supervised graph transformer on large-scale molecular data. *Advances in Neural Information Processing Systems*, 33:12559–12571, 2020.
- Vikash Sehwal, Mung Chiang, and Prateek Mittal. Ssd: A unified framework for self-supervised outlier detection. In *9th International Conference on Learning Representations*, 2021.
- Minglai Shao, Jianxin Li, Feng Chen, Hongyi Huang, Shuai Zhang, and Xunxun Chen. An efficient approach to event detection and forecasting in dynamic multivariate social media networks. In *Proceedings of the 26th International Conference on World Wide Web*, pp. 1631–1639, 2017.
- Yiyu Sun, Yifei Ming, Xiaojin Zhu, and Yixuan Li. Out-of-distribution detection with deep nearest neighbors. In *International Conference on Machine Learning*, pp. 20827–20840. PMLR, 2022.
- Petar Veličković, Guillem Cucurull, Arantxa Casanova, Adriana Romero, Pietro Liò, and Yoshua Bengio. Graph attention networks. In *International Conference on Learning Representations*, 2018.
- Shiyu Wang, Xiaojie Guo, and Liang Zhao. Deep generative model for periodic graphs. In *Advances in Neural Information Processing Systems*, 2022.
- Jim Winkens, Rudy Bunel, Abhijit Guha Roy, Robert Stanforth, Vivek Natarajan, Joseph R Ledsam, Patricia MacWilliams, Pushmeet Kohli, Alan Karthikesalingam, Simon Kohl, et al. Contrastive training for improved out-of-distribution detection. *arXiv preprint arXiv:2007.05566*, 2020.
- Jia Wu, Xingquan Zhu, Chengqi Zhang, and S Yu Philip. Bag constrained structure pattern mining for multi-graph classification. *Ieee transactions on knowledge and data engineering*, 26(10): 2382–2396, 2014.
- Qitian Wu, Yiting Chen, Chenxiao Yang, and Junchi Yan. Energy-based out-of-distribution detection for graph neural networks. In *The Eleventh International Conference on Learning Representations*, 2022.
- Zhenqin Wu, Bharath Ramsundar, Evan N Feinberg, Joseph Gomes, Caleb Geniesse, Aneesh S Pappu, Karl Leswing, and Vijay Pande. Moleculenet: a benchmark for molecular machine learning. *Chemical science*, 9(2):513–530, 2018.
- Zonghan Wu, Shirui Pan, Fengwen Chen, Guodong Long, Chengqi Zhang, and S Yu Philip. A comprehensive survey on graph neural networks. *IEEE transactions on neural networks and learning systems*, 32(1):4–24, 2020.
- Keyulu Xu, Weihua Hu, Jure Leskovec, and Stefanie Jegelka. How powerful are graph neural networks? In *International Conference on Learning Representations*, 2018.
- Kun Xu, Liwei Wang, Mo Yu, Yansong Feng, Yan Song, Zhiguo Wang, and Dong Yu. Cross-lingual knowledge graph alignment via graph matching neural network. In *Annual Meeting of the Association for Computational Linguistics*. Association for Computational Linguistics (ACL), 2019.

-
- Pinar Yanardag and SVN Vishwanathan. Deep graph kernels. In *Proceedings of the 21th ACM SIGKDD international conference on knowledge discovery and data mining*, pp. 1365–1374, 2015.
- Nianzu Yang, Kaipeng Zeng, Qitian Wu, Xiaosong Jia, and Junchi Yan. Learning substructure invariance for out-of-distribution molecular representations. In *Advances in Neural Information Processing Systems*, 2022.
- Zhitao Ying, Jiaxuan You, Christopher Morris, Xiang Ren, Will Hamilton, and Jure Leskovec. Hierarchical graph representation learning with differentiable pooling. *Advances in Neural Information Processing Systems*, 31, 2018.
- Yuning You, Tianlong Chen, Yongduo Sui, Ting Chen, Zhangyang Wang, and Yang Shen. Graph contrastive learning with augmentations. *Advances in Neural Information Processing Systems*, 33: 5812–5823, 2020.
- Ge Zhang, Zhenyu Yang, Jia Wu, Jian Yang, Shan Xue, Hao Peng, Jianlin Su, Chuan Zhou, Quan Z Sheng, Leman Akoglu, et al. Dual-discriminative graph neural network for imbalanced graph-level anomaly detection. *Advances in Neural Information Processing Systems*, 35:24144–24157, 2022.
- Muhan Zhang and Pan Li. Nested graph neural networks. *Advances in Neural Information Processing Systems*, 34:15734–15747, 2021.
- Yan Zhang, Jonathon Hare, and Adam Prugel-Bennett. Deep set prediction networks. *Advances in Neural Information Processing Systems*, 32, 2019.
- Lingxiao Zhao and Leman Akoglu. On using classification datasets to evaluate graph outlier detection: Peculiar observations and new insights. *Big Data*, 2021.
- Lingxiao Zhao, Wei Jin, Leman Akoglu, and Neil Shah. From stars to subgraphs: Uplifting any gnn with local structure awareness. In *International Conference on Learning Representations*, 2021.
- Jinhua Zhu, Kehan Wu, Bohan Wang, Yingce Xia, Shufang Xie, Qi Meng, Lijun Wu, Tao Qin, Wengang Zhou, Houqiang Li, et al. \mathcal{O} -gnn: incorporating ring priors into molecular modeling. In *The Eleventh International Conference on Learning Representations*, 2022.

APPENDIX

We provide the proof of Proposition 1 in Appendix A, more experimental details on datasets, evaluation metrics, implementation in Appendix B, several additional experiments for effectiveness, efficiency and visualization in Appendix C, and the pseudo code of SGOOD in Appendix D.

A PROOF FOR PROPOSITION 1

Proof. We first prove that SGOOD is at least as powerful as 1&2-WL in Lemma 1. Then, we prove that SGOOD can distinguish 2-regular graphs that 1&2-WL cannot distinguish in Lemma 2. Combining these two Lemmas, we prove that SGOOD is strictly more powerful than 1&2-WL. \square

Lemma 1. Let $G_1 = (V_1, E_1)$ and $G_2 = (V_2, E_2)$ be two graphs identified as non-isomorphic by 1&2-WL. SGOOD projects them into different representations \mathbf{h}_{G_1} and \mathbf{h}_{G_2} in Eq. (4).

Proof. Let $\mathcal{H}_1^G = \{\mathbf{h}_v | v \in V_1\}$ and $\mathcal{H}_2^G = \{\mathbf{h}_v | v \in V_2\}$ be the multisets of node representations of G_1 and G_2 generated by GIN in Eq. (2), respectively. Let $\mathcal{G}_1 = (\mathcal{V}_1, \mathcal{E}_1)$ and $\mathcal{G}_2 = (\mathcal{V}_2, \mathcal{E}_2)$ be the super graphs of G_1 and G_2 respectively. We consider two cases: (1) $|\mathcal{V}_1| \neq |\mathcal{V}_2|$, (2) $|\mathcal{V}_1| = |\mathcal{V}_2|$.

For case (1), \mathcal{G}_1 and \mathcal{G}_2 are two graphs with different number of nodes. Thus, \mathcal{G}_1 and \mathcal{G}_2 can be easily determined as non-isomorphic by 1&2-WL. It is proved that GIN with sufficient number of layers and all injective functions is as powerful as 1&2-WL (Xu et al., 2018). As GIN is adopted in SGOOD as GNN backbone with sufficient number of layers and READOUT function in Eq.(4) is injective, representations \mathbf{h}_{G_1} and \mathbf{h}_{G_2} of \mathcal{G}_1 and \mathcal{G}_2 are different.

For case (2), let $|\mathcal{V}_1| = |\mathcal{V}_2| = K$. Let $\mathcal{H}_1^G = \{\mathbf{h}_{g_{1,j}}^{(0)} | g_{1,j} \in \mathcal{V}_1\}$ and $\mathcal{H}_2^G = \{\mathbf{h}_{g_{2,j}}^{(0)} | g_{2,j} \in \mathcal{V}_2\}$ be the multisets of initial node representations of \mathcal{G}_1 and \mathcal{G}_2 calculated by Eq.(2), respectively. Using GIN with sufficient number of layers, we have $\mathcal{H}_1^G \neq \mathcal{H}_2^G$ (Xu et al., 2018). As stated in Section 3.1, the substructures $\{g_{i,j}\}_{j=1}^{n_i}$ of a graph G_i satisfy the following properties: (i) the substructures are non-overlapping, (ii) the union of the nodes in all substructures is the node set of G_i . Thus, $\{\{\mathbf{h}_v | v \in g_{1,j}\}_{j=1}^K\}$ (resp. $\{\{\mathbf{h}_v | v \in g_{2,j}\}_{j=1}^K\}$) is a partition of \mathcal{H}_1^G (resp. \mathcal{H}_2^G). Then, we have $\{\{\mathbf{h}_v | v \in g_{1,j}\}_{j=1}^K\} \neq \{\{\mathbf{h}_v | v \in g_{2,j}\}_{j=1}^K\}$. As POOL function in Eq.(2) is injective, we have $\{\text{POOL}(\{\mathbf{h}_v | v \in g_{1,j}\})_{j=1}^K\} \neq \{\text{POOL}(\{\mathbf{h}_v | v \in g_{2,j}\})_{j=1}^K\}$, that is $\mathcal{H}_1^G \neq \mathcal{H}_2^G$. As GIN with sufficient number of layers and READOUT function in Eq.(4) are both injective, we derive that representations \mathbf{h}_{G_1} and \mathbf{h}_{G_2} generated on \mathcal{H}_1^G and \mathcal{H}_2^G are different.

Combining case (1) and case (2), we prove Lemma 1. \square

Next, we prove that SGOOD can distinguish 2-regular graphs that 1&2-WL cannot distinguish in Lemma 2. Before that, we first give the definition of 2-regular graphs. Note that we only consider undirected graphs in this paper.

Definition 2 (2-regular graph). A graph is said to be regular of degree 2 if all local degrees are 2.

Based on the definition of a 2-regular graph, we can conclude that a 2-regular graph consists of one or more (disconnected) cycles.

Lemma 2. Given two non-isomorphic n -node 2-regular graphs $G_1 = (V_1, E_1)$ and $G_2 = (V_2, E_2)$ that 1&2-WL cannot distinguish, SGOOD projects them into different graph representations \mathbf{h}_{G_1} and \mathbf{h}_{G_2} in Eq. (4).

Proof. Based on the definition of a 2-regular graph, we can say that G_1 and G_2 consist of one or more disconnected cycles. Let r_1 and r_2 be the number of cycles in G_1 and G_2 , respectively. We consider two cases: (1) $r_1 \neq 1 \wedge r_2 \neq 1$, (2) $(r_1 = 1 \wedge r_2 \neq 1) \vee (r_1 \neq 1 \wedge r_2 = 1)$.

For case (1), G_1 and G_2 consist of disconnected circles. Let $\mathcal{G}_1 = (\mathcal{V}_1, \mathcal{E}_1)$ and $\mathcal{G}_2 = (\mathcal{V}_2, \mathcal{E}_2)$ be the constructed super graphs of G_1 and G_2 , respectively. \mathcal{G}_1 and \mathcal{G}_2 are constructed by modularity-based community detection method (Clauset et al., 2004) that assign nodes in a graph to different clusters when the modularity of the graph is maximized under such cluster assignment. As Brandes et al.

(2007) proves in Lemma 3.4, there is always a clustering with maximum modularity, in which each cluster consists of a connected subgraph. As a result, $\forall g_{1,j} \in \mathcal{V}_1$ is a circle in G_1 , and $|\mathcal{V}_1| = r_1$. Similarly, $\forall g_{2,j} \in \mathcal{V}_2$ is a circle in G_2 , and $|\mathcal{V}_2| = r_2$. Let $\mathcal{N}_1 = \{|V_{1,j}|\}_{j=1}^{|\mathcal{V}_1|}$ and $\mathcal{N}_2 = \{|V_{2,j}|\}_{j=1}^{|\mathcal{V}_2|}$. Since G_1 and G_2 are non-isomorphic, we have $\exists n_{1,j} \in \mathcal{N}_1 : \forall n_{2,j} \in \mathcal{N}_2, n_{1,j} \neq n_{2,j}$. As a result, we have $\mathcal{N}_1 \neq \mathcal{N}_2$. Then, we have $\{\{\mathbf{h}_v | v \in V_{1,j}\}\}_{j=1}^{|\mathcal{V}_1|} \neq \{\{\mathbf{h}_v | v \in V_{2,j}\}\}_{j=1}^{|\mathcal{V}_2|}$. As POOL function in Eq.(2) is injective, we have $\{\text{POOL}(\{\mathbf{h}_v | v \in g_{1,j}\})\}_{j=1}^{|\mathcal{V}_1|} \neq \{\text{POOL}(\{\mathbf{h}_v | v \in g_{2,j}\})\}_{j=1}^{|\mathcal{V}_2|}$, that is $\mathcal{H}_1^G \neq \mathcal{H}_2^G$. As GIN with sufficient number of layers and READOUT function in Eq.(4) are both injective, we have representations \mathbf{h}_{G_1} and \mathbf{h}_{G_2} generated on \mathcal{H}_1^G and \mathcal{H}_2^G are different.

For case (2), we consider $r_1 = 1 \wedge r_2 \neq 1$, and the proof when $r_2 = 1 \wedge r_1 \neq 1$ is similar. G_1 consists of one single circle, and G_2 consists of r_2 disconnected circles. Let $\mathcal{G}_1 = (\mathcal{V}_1, \mathcal{E}_1)$ and $\mathcal{G}_2 = (\mathcal{V}_2, \mathcal{E}_2)$ be the constructed super graphs of G_1 and G_2 , respectively. For G_2 and \mathcal{G}_2 , $\forall g_{2,j} \in \mathcal{V}_2$ is a circle in G_2 , and $|\mathcal{V}_2| = r_2$ following the conclusion in case (1). For G_1 and \mathcal{G}_1 , we consider two cases: (i) $|\mathcal{V}_1| = r_1 = 1$, and (ii) $|\mathcal{V}_1| > 1$. For case (i), $\mathcal{V}_1 = \{g_{1,1}\}$, where $g_{1,1} = G_1$. Let $\mathcal{N}_1 = \{|V_{1,j}|\}_{j=1}^{|\mathcal{V}_1|} = \{|V_{1,1}|\}$ and $\mathcal{N}_2 = \{|V_{2,j}|\}_{j=1}^{|\mathcal{V}_2|}$, where $|\mathcal{V}_2| > 1$. We have $\mathcal{N}_1 \neq \mathcal{N}_2$. Similar to case (1), we have the same conclusion that graph representations \mathbf{h}_{G_1} and \mathbf{h}_{G_2} generated on \mathcal{H}_1^G and \mathcal{H}_2^G are different. For case (ii), $\mathcal{V}_1 = \{g_{1,j}\}_{j=1}^{|\mathcal{V}_1|}$, where $\forall g_{1,j} \in \mathcal{V}_1$ is a chain and two nearby chain are connected in \mathcal{G}_1 . In other words, \mathcal{G}_1 is a $|\mathcal{V}_1|$ -circle while \mathcal{G}_2 consists of $|\mathcal{V}_2|$ isolated nodes. Thus, \mathcal{G}_1 and \mathcal{G}_2 can be easily distinguished as non-isomorphic by 1&2-WL. According to (Xu et al., 2018), when we encode \mathcal{G}_1 and \mathcal{G}_2 by Eq. (3) with sufficient layers of GIN, and generate \mathbf{h}_{G_1} and \mathbf{h}_{G_2} by Eq. (4), where READOUT is injective, \mathbf{h}_{G_1} and \mathbf{h}_{G_2} are different. Combining case (i) and case (ii), we prove that SGOOD generates different \mathbf{h}_{G_1} and \mathbf{h}_{G_2} for G_1 and G_2 in case (2).

Combining case (1) and case (2), we prove Lemma 2. □

B EXPERIMENTAL SETTINGS

We provide more details on datasets, evaluation metrics, and implementation here for reproducibility. All experiments are conducted on a Linux server with Intel Xeon Gold 6226R 2.90GHz CPU and an Nvidia RTX 3090 GPU card.

B.1 DATASET DETAILS

We adopt real-world datasets in various data domains for graph-level OOD detection. The dataset statistics is listed in Table 2. Following existing work (Liu et al., 2023b; Li et al., 2022b), given a graph dataset, we use graphs of the same type with distribution shift as ID and OOD data, respectively. The detailed descriptions of ID and OOD graphs in the 6 datasets are as follows.

- **ENZYMES (Morris et al., 2020)** dataset comprises protein networks representing enzymes classified into 6 EC top-level classes. In this paper, we consider graphs from *all* classes in ENZYMES as in-distribution (ID) graphs. To introduce OOD graphs, we utilize graphs from the PROTEINS dataset (Morris et al., 2020). PROTEINS is also a dataset of protein networks, where graphs are labeled as either 'Enzymes' or 'Non-enzymes'. Specifically, we use graphs in PROTEINS with label 'Non-enzymes' as OOD graphs. Consequently, the OOD graphs in ENZYMES represent unseen classes.
- **IMDB-M (Morris et al., 2020)** is a dataset of social networks. It consists of ego-networks derived from actor collaborations. The graphs are labeled with three genres: Comedy, Romance, and Sci-Fi. We consider graphs from *all* classes in IMDB-M as ID graphs. To introduce OOD graphs, we utilize graphs from another dataset called IMDB-B (Morris et al., 2020). Similar to IMDB-M, IMDB-B is also a dataset of social networks, but the graphs are labeled as either 'Action' or 'Romance'. Specifically, we use graphs labeled as 'Action' as OOD graphs. These OOD graphs do not belong to any classes in IMDB-M, and they represent unseen classes.
- **IMDB-B (Morris et al., 2020)** dataset is constructed in a similar manner to IMDB-M. Specifically, we consider graphs from *both* classes (Action and Romance) in IMDB-B as ID graphs. On the other hand, we regard graphs labeled as 'Comedy' or 'Sci-Fi' in IMDB-M as OOD graphs. These OOD graphs represent classes that are not present in IMDB-B, and they are with unseen classes.

-
- **REDDIT-12K** (Yanardag & Vishwanathan, 2015) dataset is a large-scale dataset of social networks. It consists of graphs corresponding to an online discussion thread in REDDIT where nodes correspond to users. The graphs are labeled as 11 classes based on the subreddit they belong to. In this paper, we consider graphs from *all* classes in REDDIT-12K as in-distribution (ID) graphs. To introduce OOD graphs, we utilize graphs from the REDDIT-BINARY dataset (Yanardag & Vishwanathan, 2015) where graphs also represent online discussion threads and are labeled as question/answer-based community or a discussion-based community. Consequently, the OOD graphs in REDDIT-12K represent unseen classes.
 - **BACE** (Wu et al., 2018) is a dataset of molecular graphs used for predicting particular physiology properties of chemical compounds. The dataset is split into training/validation/test sets based on the scaffolds of molecules. Notably, the samples in the training set have distinct scaffolds compared to those in the validation and test sets. The molecular properties of different scaffolds are often quite different (Ji et al., 2022). We consider graphs from the training set as ID graphs, while graphs from the test set are treated as OOD graphs. The OOD graphs exhibit a scaffold distribution that differs from ID graphs.
 - **BBBP** (Wu et al., 2018) is a dataset of molecular graphs for predicting barrier permeability. Like BACE dataset, BBBP is split into training, validation, and test sets based on the scaffolds of molecules. We consider graphs from the training set as ID graphs, while graphs from the test set are treated as OOD graphs. The OOD graphs exhibit a scaffold distribution that differs from the ID graphs.
 - **DrugOOD** is a dataset of molecular graphs generated by the dataset curator provided by (Ji et al., 2022), which is a systematic OOD dataset curator and benchmark for AI-aided drug discovery. We focus on the sub-dataset DrugOOD-sbap-core-ec50-protein, which contains molecular graphs for the task structure-based affinity prediction. The dataset is split into training/validation/test sets based on the protein target of molecules. Graphs from the training set are considered ID graphs, while graphs from the test set are treated as OOD graphs. The OOD graphs exhibit a protein target distribution that differs from that of the ID graphs.
 - **HIV** (Wu et al., 2018) is a large-scale dataset of molecular graphs for testing compounds on the ability to inhibit HIV replication. Like BACE and BBBP dataset, HIV is split into training, validation, and test sets based on the scaffolds of molecules. We consider graphs from the training set as ID graphs, while graphs from the test set are treated as OOD graphs. The OOD graphs exhibit a scaffold distribution that differs from the ID graphs.

B.2 EVALUATION METRICS

We explain in details the OOD detection evaluation metrics. We use three commonly-used metrics AUROC, AUPR and FPR95 for OOD detection evaluation (Hendrycks & Gimpel, 2017; Wu et al., 2022). All the three metrics are independent of threshold choosing.

- **AUROC**, short for Area Under the Receiver Operating Characteristic (ROC) Curve, is a widely used performance metric. It quantifies the area under the ROC curve, which plots the True Positive Rate (TPR) against the False Positive Rate (FPR) across different probability thresholds ranging from 0 to 1. The AUROC score provides a comprehensive assessment of a model’s ability to differentiate between the positive and negative classes, reflecting its overall discriminative power.
- **AUPR** stands for Area Under the Precision-Recall Curve. Precision-Recall curve is a plot of precision versus recall at various probability thresholds ranging from 0 to 1. Higher AUPR indicates that positive samples are correctly identified while false positive predictions are minimized. AUPR is particularly useful in imbalanced datasets where one class is significantly underrepresented compared to the other.
- **FPR95** stands for False Positive Rate at 95% True Positive Rate. FPR95 measures the false positive rate (FPR) when the true positive rate (TPR) is 95%. A lower FPR95 value indicates better performance, as it means the classifier is able to maintain a high true positive rate while minimizing false positive predictions.

B.3 IMPLEMENTATION DETAILS OF BASELINES

We provide more description and implementation details of the baselines in Section 4.

-
- **MSP, Energy, ODIN** are general OOD detection methods that estimate OOD scores directly from classification logits at test time. Specially, MSP (Hendrycks & Gimpel, 2017) is the first and the most basic baseline that directly uses the maximum softmax score as OOD score. Energy (Liu et al., 2020) uses energy function that works directly on the output logits to predict OOD scores. ODIN (Liang et al., 2018) uses temperature scaling with gradient-based input perturbations to enlarge the outputs differences between OOD and ID samples.
 - **MAH** (Lee et al., 2018) is a distance-based OOD detection method. It models the feature embedding space as a mixture of multivariate Gaussian distributions and measures OOD scores according to the MAH distance between test samples and ID training data.
 - **GNNSafe** (Wu et al., 2022) is a graph OOD detection method based on energy model. It incorporates GNNs in the energy model and detects OOD samples using energy scores. For node-level OOD detection, it further adopts a propagation scheme to leverage graph structure through unlabeled nodes. In our paper, we use graph labels to directly run the basic version of GNNSafe from its Section 3.1 (Wu et al., 2022).
 - **GraphDE** (Li et al., 2022b) is a graph-level OOD detection method based on probabilistic model. It addresses both the challenges of debiased learning and OOD detection in graph data. By modeling the graph generative process and incorporating a latent environment variable, the model can automatically identify outliers during training and serve as an effective OOD detector.
 - **GOOD-D** (Liu et al., 2023b) is an unsupervised graph-level OOD detection method. It detects OOD graphs solely based on unlabeled ID data. GOOD-D utilizes a graph contrastive learning framework combined with perturbation-free graph data augmentation to capture latent ID patterns and detect OOD graphs based on semantic inconsistency at multiple levels of granularity.
 - **OCGIN** (Zhao & Akoglu, 2021) is a graph-level anomaly detection method that combines deep one-class classification with GIN (Xu et al., 2018). It aims to project the outlier graphs at a significant distance from the training graphs in the learned feature space.
 - **OCGTL** (Qiu et al., 2022) is a graph-level anomaly detection method based on self-supervised learning and transformation learning. It develops an one-class objective that encourages graph embeddings of training data to concentrate within a hyper-sphere and outlier graphs are distant to the hyper-sphere.
 - **GLocalKD** (Ma et al., 2022) is a graph-level anomaly detection method. By training a predictor network to reproduce representations from a randomly-initialized network, the model learns both global and local normal patterns in the training data. Anomaly scores are then computed based on the prediction error, allowing the detection of irregular or abnormal graphs.

Implementation Details. For MSP, Energy, ODIN, and MAH baselines, we substitute the network backbone in their official implementation with a 5-layer GIN (Xu et al., 2018) using a fixed hidden dimension of 16 to encode graphs into node representations. The node representations from different layers are first concatenated and then aggregated using sum pooling for the final graph representations. Graph representations are sent to linear layer for classification logits. Other experimental settings are the same as SGOOD. For ODIN, as we lack auxiliary OOD data for hyperparameter fine-tuning, we initially explore the temperature values from 1, 10, 100, 1000 and the perturbation magnitudes from 0, 0.001, 0.002, 0.004 on all datasets. After experimental tuning, we set the temperature to 10 and the perturbation magnitude to 0.002 consistently achieves competitive performance across all datasets. This configuration is then fixed for further evaluation. For MAH, we leverage the graph representations used for classification to compute the MAH distance, which serves as the estimated OOD scores. However, we do not employ the calibration techniques, such as input pre-processing and feature ensemble in the original paper (Lee et al., 2018). We observed a significant drop in performance when implementing MAH with these techniques. We guess the reason is that the calibration techniques designed for image data are not suitable for graphs. For the other competitors, we use their original codes provided by the respective authors. All competitors are trained using ID training graphs and fine-tuned using ID graphs in validation set.

C ADDITIONAL EXPERIMENTS

Performance on ID graph classification. Table 9 reports the performance on ID graph classification of all methods by Accuracy (ID ACC). We observe that SGOOD achieves best ID ACC on 7/8 datasets, which indicates that leveraging substructures also benefits graph classification. Nevertheless, note that, as mentioned, the main goal of OOD detection is to accurately identify OOD data during testing, while maintaining instead of significantly improving ID ACC.

Table 9: ID graph classification performance measured by ID ACC. All results are reported in percentage % (mean \pm std). / indicates that ID ACC is not applicable for unsupervised methods.

Method	ENZYMES	IMDB-M	IMDB-B	REDDIT-12K	BACE	BBBP	HIV	DrugOOD
MSP	37.33 \pm 8.73	48.27 \pm 3.58	69.80 \pm 5.38	48.91 \pm 1.06	80.83 \pm 2.41	87.44 \pm 2.57	96.62 \pm 0.39	79.20 \pm 6.49
Energy	37.33 \pm 8.73	48.27 \pm 3.58	69.80 \pm 5.38	48.91 \pm 1.06	80.83 \pm 2.41	87.44 \pm 2.57	96.62 \pm 0.39	79.20 \pm 6.49
ODIN	37.33 \pm 8.73	48.27 \pm 3.58	69.80 \pm 5.38	48.91 \pm 1.06	80.83 \pm 2.41	87.44 \pm 2.57	96.62 \pm 0.39	79.20 \pm 6.49
MAH	37.33 \pm 8.73	48.27 \pm 3.58	69.80 \pm 5.38	48.91 \pm 1.06	80.83 \pm 2.41	87.44 \pm 2.57	96.62 \pm 0.39	79.20 \pm 6.49
GNNSafe	17.66 \pm 2.71	30.13 \pm 5.55	50.20 \pm 2.70	27.42 \pm 6.62	56.69 \pm 8.24	79.14 \pm 11.55	96.58 \pm 0.34	64.40 \pm 20.08
GraphDE	46.00 \pm 2.70	37.86 \pm 5.89	69.80 \pm 7.05	40.68 \pm 8.64	77.68 \pm 3.65	88.90 \pm 1.00	96.20 \pm 0.40	77.00 \pm 6.39
GOOD-D	/	/	/	/	/	/	/	/
OCGIN	/	/	/	/	/	/	/	/
OCGTL	/	/	/	/	/	/	/	/
GLocalKD	/	/	/	/	/	/	/	/
SGOOD	48.66\pm3.49	48.66\pm2.77	71.60\pm3.00	51.82\pm1.51	80.33 \pm 2.84	89.14\pm3.44	96.66\pm0.29	79.40\pm3.81

Table 10: Performance with different backbones by AUROC (%). **Bold**: best. Underline: runner-up.

Backbone	Method	ENZYMES	IMDB-M	IMDB-B	BACE	BBBP	DrugOOD
GCN	MAH	70.04	71.27	53.46	72.68	54.97	66.01
	GraphDE	61.40	68.44	29.13	53.24	52.50	56.61
	GOOD-D	41.96	61.71	59.53	72.52	<u>58.91</u>	61.79
	OCGIN	64.35	57.46	64.08	67.54	51.23	59.30
	SGOOD	71.26	73.52	65.91	83.42	62.76	72.52
GraphSage	MAH	68.07	48.06	43.63	<u>73.60</u>	53.88	<u>64.55</u>
	GraphDE	61.37	69.65	28.28	53.24	52.50	56.66
	GOOD-D	45.55	57.02	23.90	73.15	<u>56.85</u>	61.57
	OCGIN	71.75	36.86	71.44	57.47	46.65	63.82
	SGOOD	<u>70.21</u>	<u>68.63</u>	<u>61.59</u>	82.22	59.50	68.60

Performance under different backbones other than GIN. We evaluate the performance of SGOOD and competitors when changing the GIN backbone to GCN (Kipf & Welling, 2017) and GraphSage (Hamilton et al., 2017). Table 10 reports the results. Observe that, with GCN backbone, compared with the baselines, SGOOD consistently achieves the best scores; with GraphSage backbone, SGOOD is the best on BACE, BBBP, DrugOOD, and the second best on other datasets. The results validate the versatility/robustness of SGOOD to different backbones.

The effect of augmentation ratio. We conduct experiments to study the effect of augmentation ratio on the three substructure-preserving graph augmentations (SD, SG, SS) introduced in Section 3.2. Specially, we fix \mathcal{T}_0 as I that indicates no augmentation, set \mathcal{T}_1 as one of the three augmentations, and vary the augmentation ratio (dropping ratio/substitution ratio) from 0.1 to 0.5. Intuitively, larger augmentation ratio leads to harder contrastive tasks. Figure 3 reports the results, and the dotted red line indicates the performance of SGOOD\CL without any augmentation for calibration. First, for all three substructure-preserving graph augmentations, under most augmentation ratio settings, we can achieve better performance than the red-dot baseline. Second, the three augmentations usually achieve the most significant performance improvement in SGOOD under moderate augmentation ratio (e.g., 0.3 and 0.4).

The effect of pretraining epochs. We conduct experiments to study the effect of pretraining epochs T_{PT} from 0 to 200. As shown in Figure 4, compared to SGOOD without first-stage pretraining ($T_{PT} = 0$), pretraining improves SGOOD’s performance. We also found that excessive pretraining can sometimes have negative effects. For example, when $T_{PT} = 200$, SGOOD’s performance

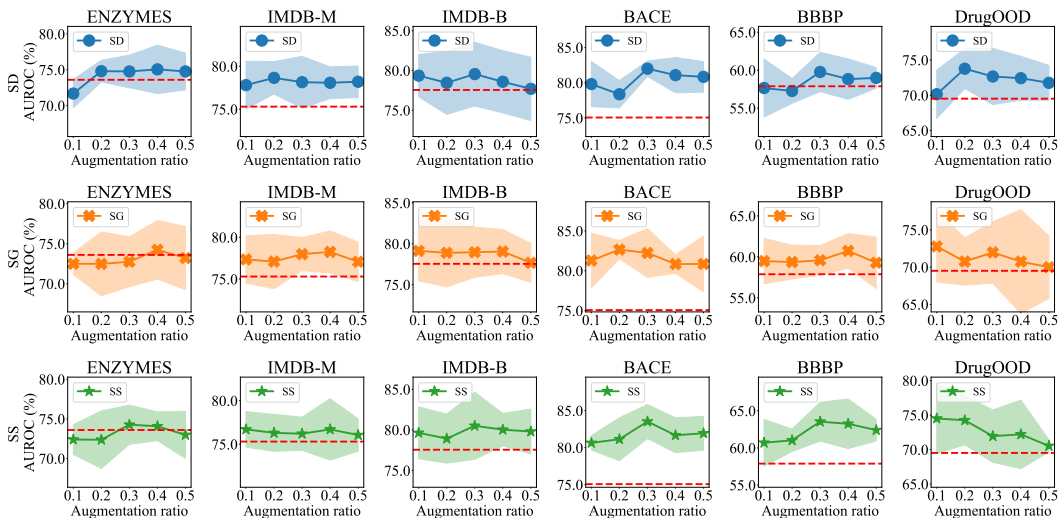


Figure 3: OOD detection performance of SGOOD when augmentation ratio varies by AUROC (%) on all the three substructure-preserving graph augmentations, SD, SG, and SS. The dotted red line indicates the performance of SGOOD\CL without any augmentation, which serves as a base performance. The area in color represents standard deviation.

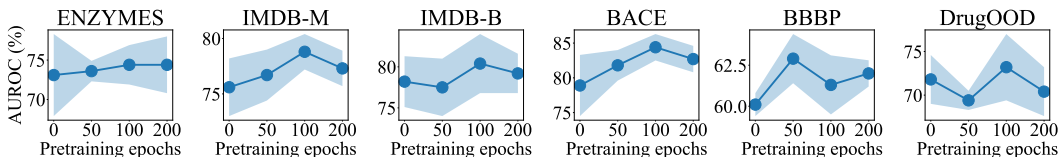


Figure 4: OOD detection performance of SGOOD by AUROC (%) when the number of pretraining epochs T_{PT} varies from 0 to 200, with colored area representing standard deviation.

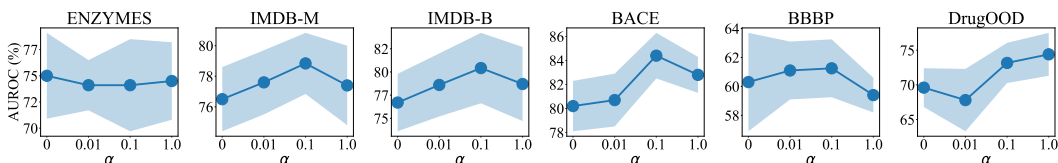


Figure 5: OOD detection results of SGOOD by AUROC (%) when the weight of the contrastive loss α varies from 0 to 1, with colored area representing standard deviation.

decrease on all datasets except ENZYMES. We speculate the reason is that excessive pretraining makes task-agnostic information dominate, with a negative impact on the SGOOD’s ability to learn from class labels. As $T_{PT} = 100$ generally leads to competitive performance across all datasets, we set the default value of T_{PT} to 100.

The effect of α . We vary the weight of the contrastive loss α from 0 to 1 to study the effect. As shown in Figure 5, compared to SGOOD fine-tuned solely by \mathcal{L}_{CE} (*i.e.*, $\alpha = 0$), fine-tuning SGOOD with both \mathcal{L}_{CE} and \mathcal{L}_{CL} generally leads to better performance. As $\alpha = 0.1$ usually leads to competitive performance across all datasets, we set the default value of α to 0.1 in SGOOD.

Visualizing pairwise combinations of all augmentations. In Figure 6, we exhaust the pairwise combinations of all options in $\mathcal{A} = \{I, SD, SG, SS\}$ and visualize the AUROC gain on graph-level OOD detection over SGOOD\A without graph augmentations. As shown in Figure 6, most combinations achieve positive gains for effective OOD detection.

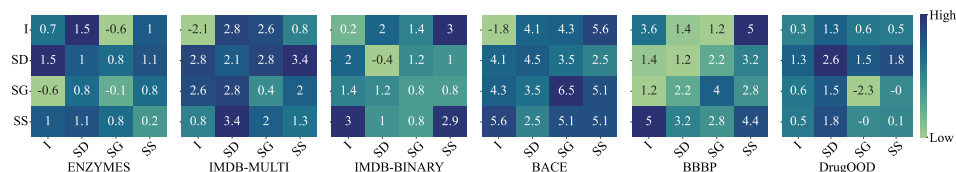


Figure 6: AUROC gain (%) of SGOOD compared with SGOOD\A without graph augmentations.

Table 11: Comparison of training time per epoch and inference time per epoch of all the methods on six datasets by seconds (s).

Method	ENZYMES		IMDB-B		IMDB-M		REDDIT-12K		BACE		BBBP		HIV		DrugOOD	
	Train (s)	Test (s)	Train (s)	Test (s)	Train (s)	Test (s)	Train (s)	Test (s)	Train (s)	Test (s)	Train (s)	Test (s)	Train (s)	Test (s)	Train (s)	Test (s)
MSP	0.119	0.008	0.090	0.007	0.077	0.007	0.890	0.260	0.053	0.005	0.055	0.006	2.740	0.200	0.078	0.005
Energy	0.119	0.008	0.090	0.007	0.077	0.007	0.890	0.260	0.053	0.005	0.055	0.006	2.740	0.200	0.078	0.005
ODIN	0.119	0.026	0.090	0.022	0.077	0.021	0.890	0.420	0.053	0.016	0.055	0.013	2.740	0.300	0.078	0.020
MAH	0.119	0.020	0.090	0.019	0.077	0.018	0.890	0.400	0.053	0.016	0.055	0.019	2.740	0.300	0.078	0.019
GraphDE	1.692	0.358	1.392	0.292	1.175	0.380	176.400	0.120	0.950	0.155	0.696	0.138	43.770	9.620	1.020	0.232
GOOD-D	0.257	0.006	0.197	0.008	0.171	0.009	17.550	0.710	0.157	0.006	0.095	0.008	5.160	0.010	0.230	0.006
OCGIN	0.123	0.005	0.086	0.006	0.079	0.005	1.650	0.170	0.075	0.005	0.044	0.005	2.900	0.050	0.099	0.005
GLocalKD	0.072	0.853	0.054	0.629	0.203	0.707	142.000	37.670	0.052	0.527	0.035	0.320	4.220	30.420	0.067	0.788
SGOOD	0.161	0.030	0.137	0.027	0.138	0.028	0.980	0.130	0.085	0.025	0.058	0.028	3.970	0.300	0.124	0.030

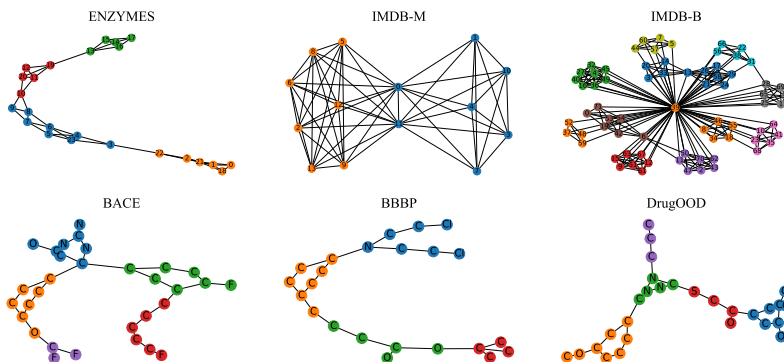


Figure 7: Different colors indicate different substructures. For molecular graphs, we label the nodes with atom types. For graphs of other types, we label the nodes with node IDs.

Model efficiency. We compare the training time per epoch and inference time per epoch in seconds of all methods, with results in Table 11. Compared with other graph-level OOD detection competitors, including GraphDE and GOOD-D, SGOOD requires less time to train. Compared with all methods, including the methods originally designed for image data, SGOOD requires moderate time for training. In terms of inference time, SGOOD is much more efficient than GraphDE. Although GOOD-D is more efficient in inference, it is not as accurate as SGOOD in OOD detection as shown in Table 3. Considering together the time cost in Table 11 and the effectiveness in Table 3, we can conclude that SGOOD has superior accuracy for graph-level OOD detection, while being reasonably efficient.

Substructure Visualization. In SGOOD, we adopt the modularity-based community detection method (Clauset et al., 2004) to detect substructures in a graph. We demonstrate the detected substructures in different datasets in Figure 7. We observe that dense cliques in protein networks (ENZYMES) and social networks (IMDB-M, IMDB-B) are separated as substructures in SGOOD. For molecular graphs, the rings that play a critical role in the properties of molecules (Zhu et al., 2022) are detected in SGOOD. As the cliques and rings can not be captured by graph representations generated by GNNs based on message passing and flat pooling (Chen et al., 2020) while SGOOD can generate substructure-enhanced graph representations, it explains why SGOOD achieves superior performance in graph-level OOD detection.

D PSEUDO-CODE OF SGOOD

We present the pseudo code of SGOOD for training and testing in Algorithm 1 and 2 respectively.

Algorithm 1: Pseudo-code of SGOOD (Training)

```
1 Input: Training dataset  $D_{tr}^{in} = \{(G_i, y_i)\}_{i=1}^n$ , testing set  $D_{test}$ , weight of the contrastive loss  $\alpha$ , number
of first-stage pretraining epoch  $T_{PT}$ , number of second-stage fine-tuning epoch  $T_{FT}$ 
// Super graph construction
2 Construct super graphs of substructures  $\{\mathcal{G}_i\}_{i=1}^n$  of all  $G_i \in D_{tr}^{in}$ ;
// First stage
3 for  $epoch = 1, 2, \dots, T_{PT}$  do
4   Randomly split training graphs  $D_{tr}^{in}$  into batches  $\mathcal{B}$  with batch size  $B$ ;
5   for  $\{G_i\}_{i=1}^B \in \mathcal{B}$  do
6     for  $G_i \in \{G_i\}_{i=1}^B$  do
7       Obtain augmented super graphs  $\widehat{\mathcal{G}}_{i,0}, \widehat{\mathcal{G}}_{i,1}$  by applying  $\mathcal{T}_0$  and  $\mathcal{T}_1$  to  $\mathcal{G}_i$ ;
8       Obtain augmented graphs  $\widehat{G}_{i,0}, \widehat{G}_{i,1}$  according to  $\widehat{\mathcal{G}}_{i,0}, \widehat{\mathcal{G}}_{i,1}$ ;
9       Calculate  $\mathbf{h}_{\widehat{\mathcal{G}}_{i,0}}$  and  $\mathbf{h}_{\widehat{\mathcal{G}}_{i,1}}$  using  $(\widehat{G}_{i,0}, \widehat{\mathcal{G}}_{i,0})$  and  $(\widehat{G}_{i,1}, \widehat{\mathcal{G}}_{i,1})$  by Eq.(1)-(4);
10      Obtain  $\mathbf{u}_{\widehat{\mathcal{G}}_{i,0}} = \frac{\psi(\mathbf{h}_{\widehat{\mathcal{G}}_{i,0}})}{\|\psi(\mathbf{h}_{\widehat{\mathcal{G}}_{i,0}})\|}$  and  $\mathbf{u}_{\widehat{\mathcal{G}}_{i,1}} = \frac{\psi(\mathbf{h}_{\widehat{\mathcal{G}}_{i,1}})}{\|\psi(\mathbf{h}_{\widehat{\mathcal{G}}_{i,1}})\|}$  using shared projection head  $\psi$  followed
by  $l_2$ -normalization;
11      Calculate contrastive loss  $\mathcal{L}_{CL}$  by Eq.(6);
12      Update parameters using mini-batch gradient descent w.r.t.  $\mathcal{L}_{CL}$ ;
// Second stage
13 for  $epoch = 1, 2, \dots, T_{FT}$  do
14   Randomly split training graphs  $D_{tr}^{in}$  into batches  $\mathcal{B}$  with batch size  $B$ ;
15   for  $\{G_i\}_{i=1}^B \in \mathcal{B}$  do
16     for  $G_i \in \{G_i\}_{i=1}^B$  do
17       Same as Lines 7-10 ;
18       Calculate  $\mathbf{h}_{G_i}$  using  $(G_i, \mathcal{G}_i)$  by Eq.(1)-(4);
19       Calculate prediction logits  $\widehat{y}_i$  by applying linear transformation on  $\mathbf{h}_{G_i}$ ;
20     Calculate cross-entropy loss  $\mathcal{L}_{CE}$  by Eq.(5);
21     Calculate contrastive loss  $\mathcal{L}_{CL}$  by Eq.(6);
22     Update parameters using mini-batch gradient descent w.r.t.  $\mathcal{L}_{CE} + \alpha\mathcal{L}_{CL}$ ;
// Estimate class centroids and covariance matrix
23 for  $G_i \in D_{tr}^{in}$  do
24   Calculate  $\{\mathbf{h}_v | v \in V_i\}$  and  $\mathbf{h}_{G_i}$  using  $(G_i, \mathcal{G}_i)$  by Eq.(1)-(4);
25   Calculate  $\mathbf{h}_{G_i} = \text{READOUT}(\{\mathbf{h}_v | v \in V_i\})$ ;
26   Calculate  $\mathbf{z}_i = \frac{\text{CONCAT}(\mathbf{h}_{G_i}, \mathbf{h}_{G_i})}{\|\text{CONCAT}(\mathbf{h}_{G_i}, \mathbf{h}_{G_i})\|_2}$ ;
27 Calculate estimated class centroids  $\{\boldsymbol{\mu}_c\}_{c=1}^C$  and covariance matrix  $\widehat{\Sigma}$  by Eq.(9);
```

Algorithm 2: Pseudo-code of SGOOD (OOD Detection During Testing)

```
1 Input: The trained SGOOD model  $f$ , testing set  $D_{test}$ , estimated class centroids  $\{\boldsymbol{\mu}_c\}_{c=1}^C$ , estimated
covariance matrix  $\widehat{\Sigma}$ 
// Testing stage
2 for  $G_i \in D_{test}$  do
3   Construct super graph  $\mathcal{G}_i$ ;
4   Calculate  $\{\mathbf{h}_v | v \in V_i\}$  and  $\mathbf{h}_{G_i}$  using  $(G_i, \mathcal{G}_i)$  and  $f$  by Eq.(1)-(4);
5   Calculate  $\mathbf{h}_{G_i} = \text{READOUT}(\{\mathbf{h}_v | v \in V_i\})$ ;
6   Calculate  $\mathbf{z}_i = \frac{\text{CONCAT}(\mathbf{h}_{G_i}, \mathbf{h}_{G_i})}{\|\text{CONCAT}(\mathbf{h}_{G_i}, \mathbf{h}_{G_i})\|_2}$ ;
7   Calculate OOD score  $S(G_i)$  by Eq.(8);
8   if  $G_i$  is not OOD based on  $S(G_i)$  then
9     Perform classification on  $G_i$  via prediction logits  $\widehat{y}_i$  by applying linear transformation on  $\mathbf{h}_{G_i}$ ;
```
